Doctoral Dissertation (Censored)

博士論文 (要約)

Biochemical and structural studies on the nucleosome recognition mechanism by the pioneer transcription factor p53

(パイオニア転写因子 p53 によるヌクレオソーム認識機構の

生化学的・構造生物学的解析)

A Dissertation Submitted for the Degree of Doctor of Philosophy

December 2021

令和 3 年 12 月博士(理学)申請

Department of Biological Sciences, Graduate School of Science,

The University of Tokyo

東京大学大学院理学系研究科生物科学専攻

Masahiro Nishimura

西村　正宏

Contents

Figures and Tables

Abstract

In eukaryotes, the genomic DNA is accommodated into the nucleus, forming a chromatin structure with nucleosomes as a basic unit. The nucleosome is a disk-shaped structure, in which histone octamer containing two molecules each of the histone proteins H2A, H2B, H3, and H4, is wrapped by about 145 base-pairs of DNAs. The extended DNA regions connecting adjacent nucleosomes are termed linker DNA. The nucleosome structure inherently inhibits the transcription factors' binding to the genomic DNA, therefore, regulating transcription. On the other hand, a subset of transcription factors termed "pioneer transcription factors" can bind to the target DNA sequence within the nucleosome and induce chromatin opening. The ability of pioneer transcription factors to bind to nucleosomes is indispensable in regulating cell fate, but the detailed molecular mechanism is still unknown. As a pioneer transcription factor, p53; a major protein involved in tumor suppression, induces the expression of genes involved in cell cycle arrest and apoptosis in response to various cellular stresses. However, previous crystallographic studies of the p53-DNA complexes revealed that the structure of the p53 bound DNA containing the p53 target sequence was a straight path. In this study, the mechanism of nucleosomal DNA recognition by p53 was investigated through biochemical and structural analysis using recombinant proteins.

The gel shift assay showed that linker DNAs portions are required for the formation of p53-nucleosome complexes that appeared as four discrete bands on the polyacrylamide gel. The insertion of the p53 binding sequence into the nucleosomal DNA, which mimics natural p53 binding sites in the context of chromatin, did not significantly affect the nucleosome binding efficiency, meanwhile, p53 formed an additional specific complex with the nucleosome in the presence of the p53 binding sequence. In addition,

the pull-down experiment and the gel shift assay revealed that p53 directly binds to the histone H3-H4 complex via its N-terminal amino acid region. The cryo-EM analysis of the p53-nucleosome complex was then performed and revealed that p53 bound to the target sequence within the nucleosome. The hydroxy-radical footprinting experiments also support the p53-DNA interactions within the p53-nucleosome structure.

These results provide basic information on how p53 binds to the nucleosome and insight into the underlying mechanism of how pioneer transcription factors induce chromatin opening.

Abbreviations

Abbreviation	Full name
bp	base-pair
CBB	Coomassie brilliant blue
cryo-EM	cryo-electron microscopy
CTF	contrast transfer function
CV	Column volume
DNA	Deoxyribonucleic acid
DNase Ⅰ	Deoxyribonuclease Ⅰ
DTT	Dithiothreitol
EDTA	ethylenediaminetetraacetic acid
EMSA	electrophoretic mobility shift assay
EtBr	Ethidium bromide
FRAP	fluorescence recovery after photobleaching
FSC	Fourier shell correlation
GS4B	Glutathione Sepharose 4B
GST	Glutathione S- transferase
HEPES	4-(2-hydroxyethyl)-1-piperazineethanesulfonic acid
IPTG	Isopropyl β-D-1-thiogalactopyranoside
LB	Luria-Bertani
MNase	Micrococcal Nuclease
MWCO	molecular weight cut-off
Ni-NTA	Nickel-nitrilotriacetic acid
NP-40	Nonidet P-40
PAGE	Polyacrylamide gel electrophoresis
PCI	Phenol/chloroform/isoamyl alcohol
PCR	Polymerase chain reaction
ProK	Proteinase K
RNA	Ribonucleic acid
rpm	rotate per minutes
SDS	Sodium dodecyl sulfate

TBE	Tris/Borate/EDTA
TCEP	tris(2-carboxyethyl)phosphine
Tris	tris(hydroxymethyl)aminomethane
Urea-PAGE	Urea denaturing polyacrylamide gel electrophoresis
β-me	β-mercaptoethanol

Chapter 1: General introduction

1.1 Chromatin structure and function

Eukaryotes exhibiting complex multicellular systems have evolved larger genomes than prokaryotes (1, 2). For example, in humans, about 6.2 billion bps of diploid genome DNA (about 2 m in total length) are accommodated into a nucleus with a diameter of only about 5-8 μm (3). Such a highly folded organization of the genomic DNA is precisely regulated along with cell cycle, which was first described and named "chromatin" by Flemming Walther in 1882 (4). About 90 years later, the structure of chromatin was first revealed as "beads-on-a-string" by the electron microscopy observations (5–7). The basic repeating unit of chromatin is then termed nucleosome, and the DNA regions connecting the adjacent nucleosomes are termed linker DNA: each of them corresponds to the "beads" or "string", respectively (Figure 1-1 A).

Crystallographic studies have shown the detailed structure of the nucleosome, in which a 145-147 bp length of DNA wrapped around a histone core containing two copies of each four core histones, H2A, H2B, H3, and H4 (8–11) (Figure 1-3 B). In the structure of a nucleosome, a histone H3-H4 tetramer and two histone H2A-H2B dimers interact with each other to form an octameric histone core and organize its nucleosomal DNA. Each location of nucleosomal DNA is terminologically designated by "superhelical location (SHL)", numbered from SHL(0) at the center to SHL(±7) at both edges in 10 bp intervals (Figure 1-1 C). The backbone moieties of the nucleosomal DNA between each SHL periodically interact with the histone core surfaces (12). As long as revealed so far, the overall structures of the nucleosomes are widely conserved among species, including *Homo sapiens* (13), *Mus musculus* (14), *Gallus gallus* (9), *Xenopus laevis* (8), *Drosophila melanogaster* (15), *Saccharomyces cerevisiae* (16),

Giardia lamblia (17). Consistently, nucleosome organizations (18–24) and nucleosome binding motifs within epigenetic regulators such as chromatin remodeler SWI/SNF family (25–27) are also evolutionally conserved.

Chromatin structure inherently restricts the DNA access by various factors involved in transcription such as RNA polymerases (28–31) and transcription factors (32–35); therefore, enzymatically accessible chromatin region: open chromatin is considered to be transcriptionally active (36–38) (Figure 1-1 D). Consequently, the alterations of the nucleosome structure mediated by the inherent dynamics and nucleosome binding factors profoundly affect genome functions (39–41). The nucleosome itself adopts dynamic nature regarding composition and conformation (Figure 1-1 E). As for composition, the histones in the nucleosome can be replaced by their non-allelic isoforms, termed histone variants (42). Incorporation of the histone variants confers the structural characterization and the interaction property of the nucleosome, thereby playing significant roles in the regulation of chromatin (43). Post-transcriptional modification of histones also plays a crucial role in epigenetic regulation. The intrinsically disordered N-terminal amino acid regions in histones so-called histone tails are often targeted by the specific methylation, acetylation, phosphorylation in the various biological context including development, differentiation, and cell cycle (44, 45). As for conformation, the nucleosomal linker DNAs can be transiently released from the histone (46, 47). Such dynamic nature, termed “nucleosome breathing” may also potentiate chromatin dynamics and epigenetic regulations (47–49).

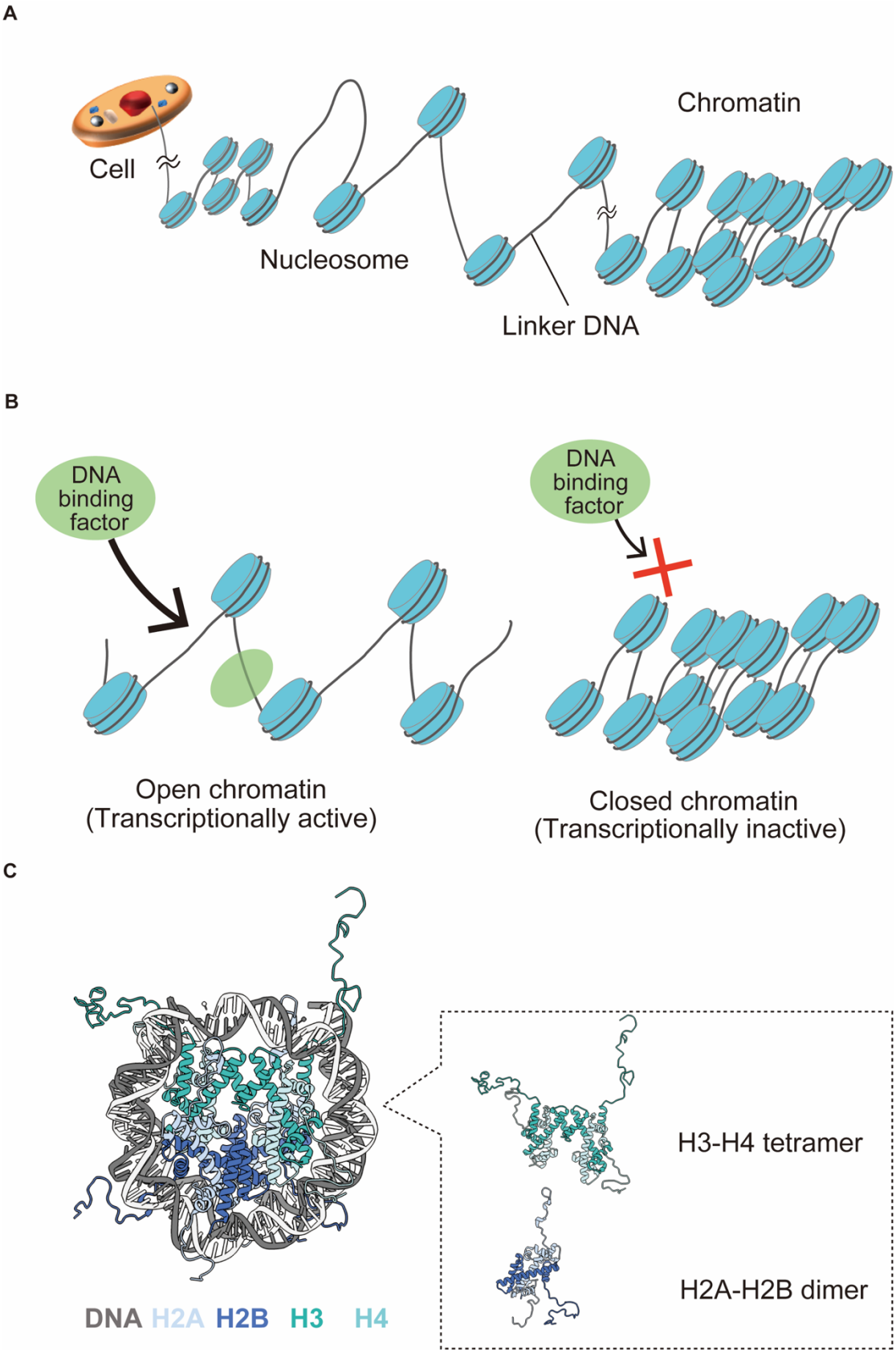
A
Cell
Chromatin
Nucleosome
Linker DNA
B
DNA binding factor
DNA binding factor
Open chromatin
(Transcriptionally active)
Closed chromatin
(Transcriptionally inactive)
C
DNA H2A H2B H3 H4
H3-H4 tetramer
H2A-H2B dimer

D

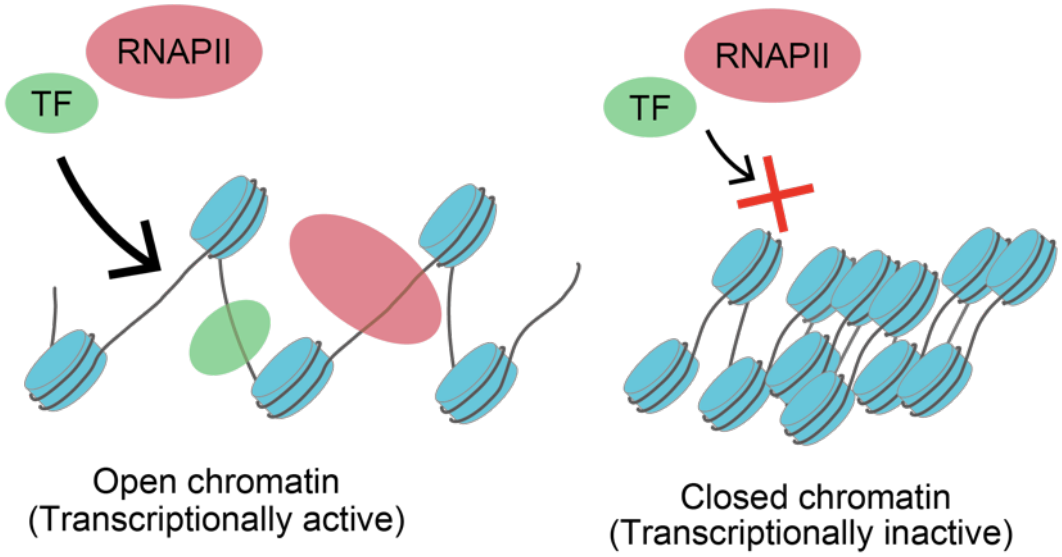
RNAPII
TF
Open chromatin
(Transcriptionally active)
RNAPII
TF
Closed chromatin
(Transcriptionally inactive)

E

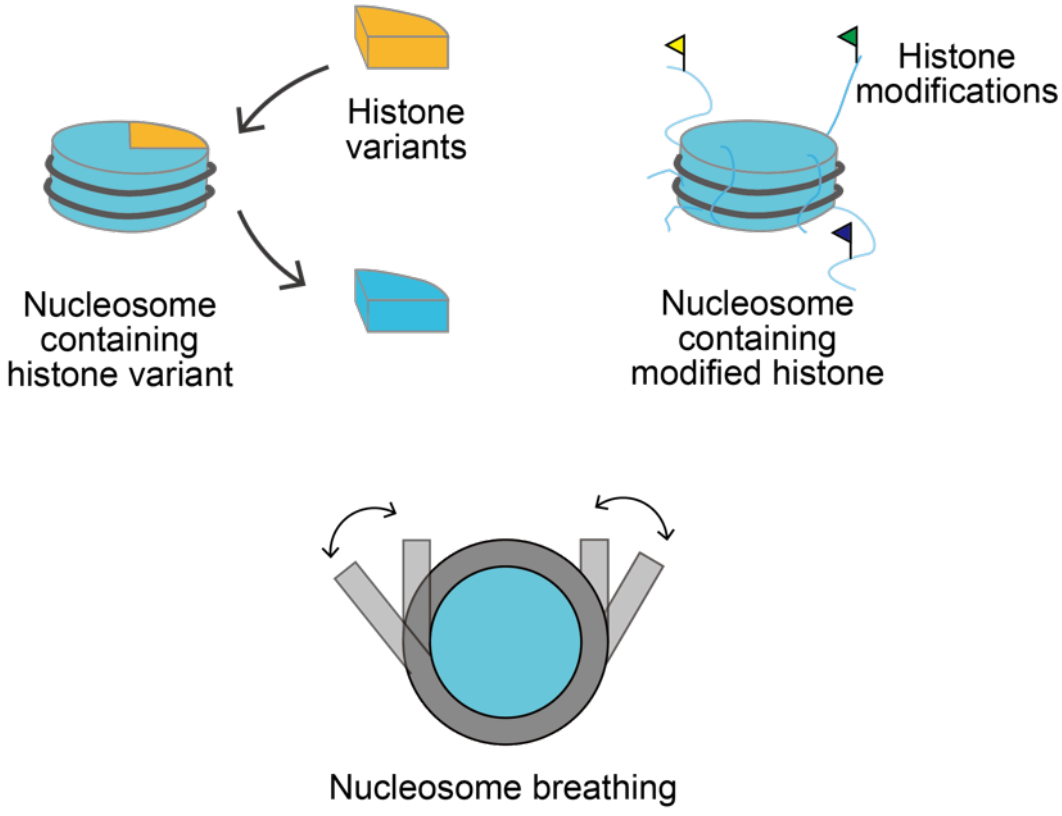
Histone
variants
Nucleosome
containing
histone variant
Histone
modifications
Nucleosome
containing
modified histone
Nucleosome breathing

Figure 1-1 Chromatin and nucleosome structures and regulations

(A) Illustration of chromatin structure.

(B) Nucleosome structure depicted by ChimeraX software (PDB ID: 1KX5). The DNA, H2A, H2B, H3, and H4 are colored in grey, light steel blue, royal blue, light sea green, and pale turquoise, respectively. The histone H3-H4 tetramer and the H2A-H2B dimer extracted from the nucleosome structure are shown in a dotted square.

(C) The structure of nucleosomal DNA, in which each SHL seen from the front is indicated on the DNA structure while the second half of the sequence is shown transparently.

(D) Illustrations of chromatin function that regulates the DNA access by DNA binding factors.

(E) Graphic explanation of the incorporations of histone variant into a nucleosome, histone modification, and nucleosome breathing.

1.2 Pioneer transcription factor

In response to internal and external stimuli, cells exhibit appropriate gene expressions to maintain homeostasis; the gene expression level is normally encoded by the regulatory sequence of the genes such as promoter, enhancer, or silencer. The readout of the regulatory sequence is assumed by a group of proteins called transcription factors that are termed by the capability to bind their specific DNA sequence and regulate transcription (50–52). Indeed, each transcription factor shares evolutionally conserved DNA-binding domains, that can typically confer 1000-fold or greater affinity to the specific DNA sequence (53, 54). Besides, among metazoans, the DNA sequence of regulatory regions, DNA-binding domains of transcription factors, and their functions are not so far from each other, implying that the gene regulatory network has been conserved over species (55, 56).

A series of genomic and biochemical studies demonstrated the role of the nucleosome, that inhibits the genomic DNA bindings by RNA polymerases (28–31) and transcription factors (32–35). In contrast, a subset of transcription factors so-called "pioneer transcription factor" is capable of binding nucleosomal DNA (57–59) (Figure 1-2). The concept of the pioneer transcription factors was established through the study of the transcription factor that had initially bound to a liver-specific enhancer during embryogenesis (60–62). As the first pioneer factors, FoxA and GATA transcription factors were identified by *in vivo* footprint experiment by Dr. Zaret Kenneth and colleagues (63). Subsequent biochemical studies showed FoxA1 and GATA4 proteins were capable of recognizing and opening the target site on nucleosomes reconstituted *in vitro* (64–67). Later, similar genetic and biochemical characteristics were found in other transcription factors involved in cellular reprogramming such as Yamanaka

factors (68–70), development (71–76), circadian rhythm (77). Until now, we have known up to 20-30 kinds of the pioneer transcription factors, that contain diverse DNA binding motifs (78–80). Recent studies about pioneer transcription factors discovered that the malfunctions of pioneer transcription factors due to somatic mutations and chromosomal translocations are attributed to many types of cancer drivers, therefore mechanisms of which each of pioneer transcription factors recognized their binding sequence embedded in the nucleosome structure gathers keen interest (81–84).

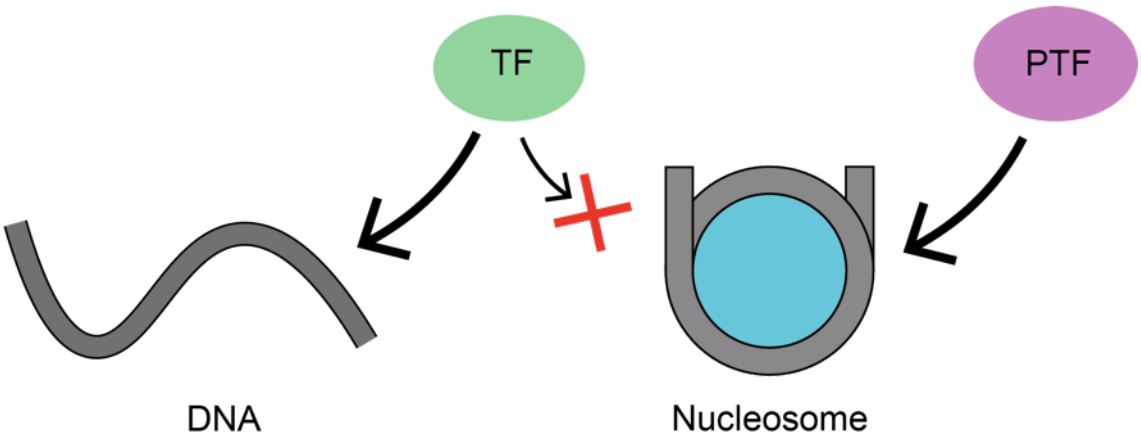

Figure 1-2 Pioneer transcription factors can bind nucleosome

Graphic explanation of the pioneer transcription factors' function. The green oval represents typical transcription factor (TF) and the purple oval represents pioneer transcription factor (PTF). Pioneer transcription factors can bind nucleosomes while transcription factors cannot.

1.3 Tumor suppressor p53

Tumor suppressor p53 functions as a transcription factor, activated in response to genotoxic stress to facilitate the expression of various genes involving cell cycle arrest, apoptosis, senescence, and DNA repair, thereby controlling cell survival and death (85) (Figure 1-3 A). The human p53 protein composes 393 amino acid residues, which include transcription activation domains 1 and 2 (TAD1, 1-40 amino acid residues; TAD2, 41-60 amino acid residues), the proline-rich region (PRR, 61-93 amino acid residues), the core DNA-binding domain (DBD, 102-293 amino acid residues), the tetramerization domain (TD, 323-353 amino acid residues), and the C-terminal domain (CTD, 364-393 amino acid residues) (86) (Figure 1-3 B). Two TADs within the N-terminal amino acid region autonomously function (87–89) and interact with various transcriptional co-factors including general transcription factors, the mediator complex, and histone-modifying enzymes such as CBP/p300 (90). The target sequence recognition is mediated by structurally conserved DBD. Mutations in the p53-coding gene, *TP53*, occur in about half of the cancer patients, especially most of the mutations accumulate within the DBD, suggesting that disruptions of p53-mediated DNA recognition may drive cancer (91–93). Unlike typical transcription factors, p53 protein has a strong sequence-nonspecific DNA binding ability mediated by CTD (94). Biochemical and single-molecule experiments suggest that p53 slides along DNA via its CTD while scanning the target sequence, meanwhile the sequence-specific DNA binding by DBD undergoes efficiently (95–98).

In the context of chromatin, p53 functions as a pioneer transcription factor, that can bind to the nucleosome (99–103) (Figure 1-3 C). Notably, previous

crystallographic studies have revealed that the structure of the target DNA in complex with the homo-tetrameric p53DBD is a linear conformation. (104–108) (Figure 1-3 D). In the structure of the p53-DNA complex, two dimers of p53DBD bind to the continuous two decameric half-sites composing “RRRCWWGYYY” (R: A or G; W: A or T; Y: C or T) (109, 110). Genomic mapping studies of the p53 localization and nucleosome positioning indicated that the p53 binding sequences reside around SHL(±7) that would be partially wrapped by histone core (100, 111), therefore p53 binding to the target DNA within the nucleosome necessitates structural alterations of either nucleosome or p53.

In this thesis, biochemical and structural studies are employed to study how p53 interacts with the nucleosomes, whose DNA sequences include or exclude the p53 binding sequence.

A

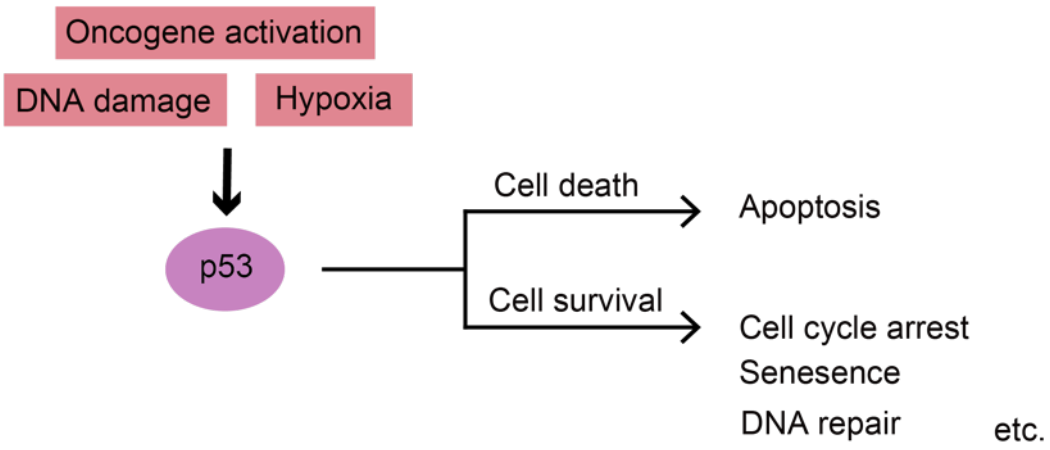
Oncogene activation
DNA damage
Hypoxia
p53
Cell death
Apoptosis
Cell survival
Cell cycle arrest
Senesence
DNA repair
etc.

B

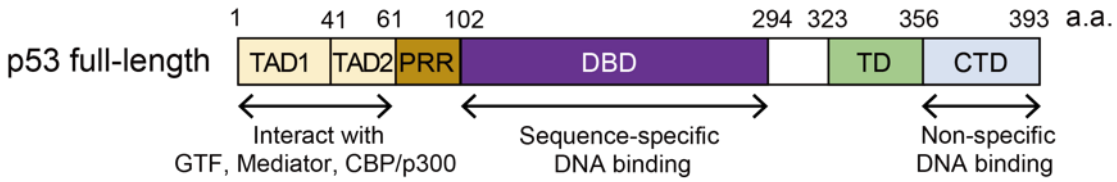
p53 full-length
1
41
61
102
294
323
356
393
a.a.
TAD1
TAD2
PRR
DBD
TD
CTD
Interact with
GTF, Mediator, CBP/p300
Sequence-specific
DNA binding
Non-specific
DNA binding

C

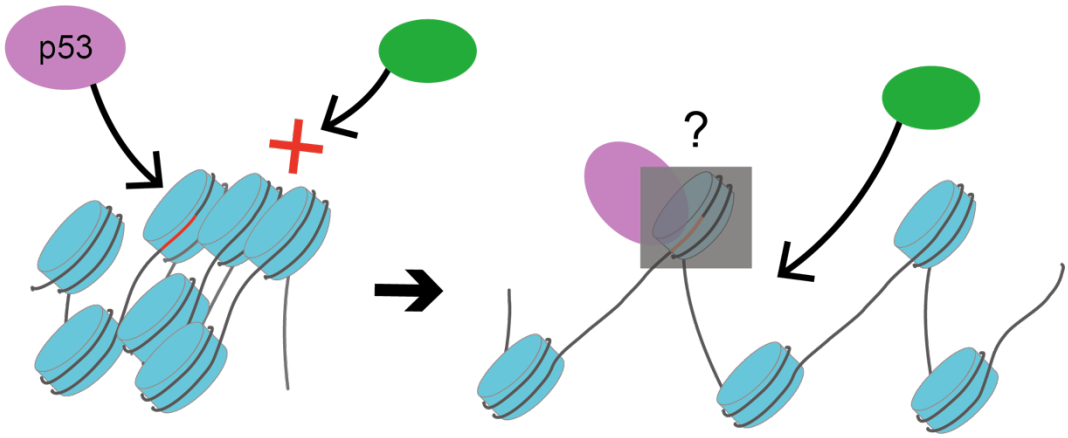
p53
?
Closed chromatin
(Transcriptionally inactive)
Open chromatin
(Transcriptionally active)

D

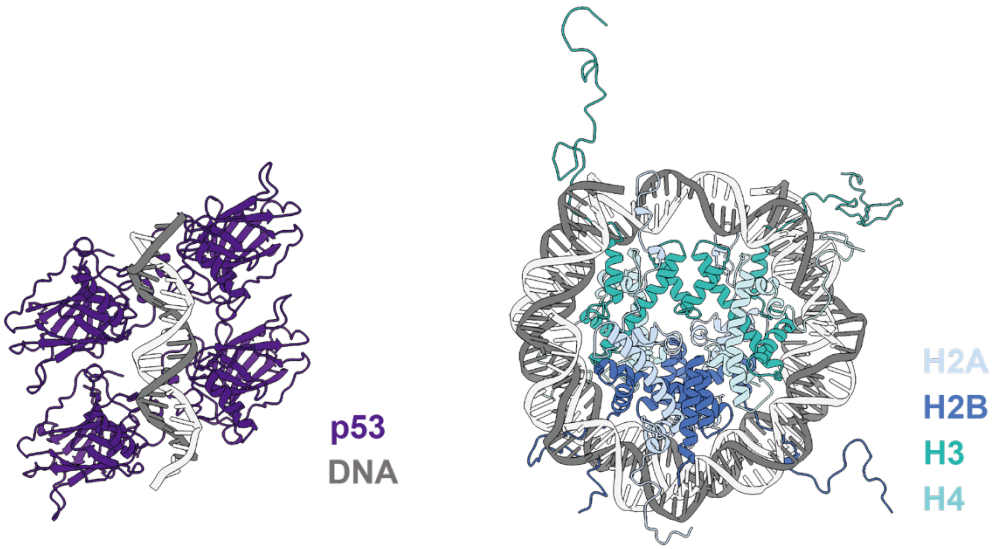
p53
DNA
H2A
H2B
H3
H4
p53DBD-DNA complex
Nucleosome

Figure 1-3 Structure and function of p53

(A) Schematic illustration of the genotoxic stress-induced p53 activation selects cell fate through p53 target genes.
(B) Domain structure of the human p53 protein. Transcription activation domains 1 and 2 (TAD1/2), proline-rich region (PRR), core DNA-binding domain (DBD), tetramerization domain (TD), and C-terminus domain (CTD) are indicated.
(C) Graphic explanation of the pioneering activity of p53. Closed chromatin regions become accessible for DNA-binding factors when the p53 is bound to the target sequence within the nucleosome.
(D) Structures of p53-DNA complex (PDB ID: 3KMD) and nucleosome (PDB ID:1KX5) are depicted by ChimeraX software. The p53, DNA, H2A, H2B, H3, and H4 are colored in indigo, grey, light steel blue, royal blue, light sea green, and pale turquoise, respectively.

Chapter 2: Materials and methods

2.1 Expression and purification of human p53

Human p53 (Uniprot ID: Q761V2) was produced in the *Escherichia coli* BL21(DE3) cells. To prepare the plasmid DNA, the DNA fragment encoding the codon-optimized p53 gene was inserted into the pGEX6P1 vector (Cytiva). The bacteria were grown in the 2 L of LB medium at 37ºC until the optical density at a wavelength of 600 nm reached 1.2 and the medium was then cooled on ice. The expression of the GST-tagged p53 protein was induced by adding 0.5 mM of IPTG, and the cells were further cultured at 18°C overnight. After 24 hours of the culture, the cells were harvested by centrifugation and resuspended in buffer 1. The resuspended cells were disrupted by sonication, and the lysates were centrifuged to collect the supernatants containing GST-tagged p53 protein. The supernatants were gently mixed with GS4B beads (Cytiva) at 4ºC for 1 hr. The beads were then loaded into an open column (Bio-Rad) followed by washing with 20 CV of buffer 2 and 20 CV of buffer 3. The elution and the tag removal were simultaneously performed by adding PreScission protease (Cytiva) and rotating the beads at 4°C overnight. The p53 protein was then purified by Heparin Sepharose (Cytiva) chromatography by stepwise elution with buffer 4 to remove co-eluted nucleic acids. The p53 protein was further purified by size-exclusion column chromatography with buffer 5. The eluted fractions were concentrated, flash-frozen, and stored at -80ºC.

For the bait of the pull-down assay, GST-tagged p53 was prepared by the same method described above until the GS4B beads (Cytiva) binding. The GST-tagged human p53 was eluted by the GST elution buffer 6. The elution was further purified by size-

exclusion column chromatography with buffer 5. The eluted fractions were concentrated, flash-frozen, and stored at -80ºC.

2.2 Purification of the human core histones and the histone complexes

The human core histone H2A (Uniprot ID: P04908), H2B (Uniprot ID: P06899), H3.1 (Uniprot ID: P68431), H4 (Uniprot ID: P62805) were prepared by the method previously described (112). In brief, the H2A, H2B, H3.1, and H4 were produced in the *Escherichia coli* cells as the N-terminally His_6-tagged proteins. The cells were disrupted by sonication, after that the His_6-tagged histones were collected from the insoluble fraction of the lysates under the denaturing condition. The sample purification was then performed by Ni-NTA agarose chromatography (QIAGEN) followed by thrombin protease cleavage and cation exchange chromatography. The purified histones were dialyzed against water and stored as a freeze-dried powder at 4ºC.

The histone H3-H4 complex for the pull-down assay and the histone octamer for the nucleosome reconstitution were prepared by the refolding method (112). In brief, the freeze-dried histones were mixed at an equal molar ratio under denaturing conditions. The histone mixtures were then refolded by dialysis and subsequently purified by size-exclusion column chromatography. The final samples were flash-frozen and stored at -80ºC.

2.3 Preparation of DNA fragments

The DNA fragments for the nucleosome reconstitutions were prepared by PCR amplification followed by the non-denaturing PAGE purification using a Prep Cell apparatus (Model 491 Prep Cell, Bio-Rad). Their DNA sequences were originated from the so-called Widom 601 sequence, which has strong nucleosome positioning property (113). As for the nucleosomal DNA containing the p53 binding sequence, the optimal DNA sequence for p53 binding, "5'-GGGCATGTCCGGGCATGTCC-3'" (114) was inserted into the nucleosome edge of the Widom 601 sequence to mimic the target nucleosome of p53.

The 24 bp DNA for the competition assay was prepared by annealing using the pair of complemental DNA primers, which were commercially obtained. The DNA sequence is identical to the linker DNA portion of the 193 bp nucleosome.

2.4 Reconstitution and purification of nucleosomes

The nucleosomes were reconstituted by the salt dialysis method as previously described (112, 115). Briefly, a DNA fragment was mixed with the purified histone octamer and then dialyzed against the reconstitution buffer, whose salt concentration gradually decreased by buffer exchange. The reconstituted nucleosome was further purified by the non-denaturing PAGE using a Model 491 Prep Cell apparatus (Bio-Rad). The purified nucleosome was eluted with buffer 7. The final sample was flash-frozen and stored at -80ºC.

2.5 EMSA for nucleosome binding by p53

To evaluate nucleosome binding by p53, 0.1 μM of nucleosomes were mixed with either 0, 0.2, 0.4, 0.6, or 0.8 μM of p53 or that of p53 mutant, in buffer 8 or buffer 9. The mixtures were incubated at 25°C for 30 minutes and were then electrophoresed on the non-denaturing 5% PAGE. The mobility shifts of the nucleosomes were visualized by EtBr staining.

2.6 2-dimensional gel analysis of the p53-nucleosome complexes

To examine protein components of each p53-nucleosome complex that appeared on the polyacrylamide gel, 60 pmol of the nucleosome and 270 pmol of p53 were mixed and were incubated in buffer 10 at 25°C for 30 min. The mixed sample was then electrophoresed on 5-12% gradient non-denaturing polyacrylamide gel (FUJIFILM Wako Pure Chemical Corporation) followed by EtBr staining. The gel was then soaked and gently agitated at room temperature for an hour, in buffer 11. The gel was then analyzed by 18% SDS-PAGE, and the protein compositions were visualized by Oriole (Bio-Rad) staining.

2.7 Assay for p53 competitive bindings to the nucleosome

To evaluate the stability of the p53-nucleosome complexes in the presence of the excess amount of the competitor DNA, 0.1 μM of the nucleosome was first mixed with 0.8 μM of p53 in buffer 8. After 30 minutes of incubation at 25ºC, either 0, 0.1, 0.2, 0.4, 0.8, or 1.6 μM of the 24 bp DNA was then added to the mixture, and further incubated at 25°C for 30 minutes. Thereafter, the samples were analyzed by the

biphasic (5/12%) non-denaturing PAGE. The retention of the p53-nucleosome complexes was visualized by EtBr staining.

2.8 EMSA for PL2-6 binding to nucleosome

To confirm the nucleosome composition, 0.1 μM of the nucleosome was mixed with 0.8 μM of p53 in buffer 8. After 30 minutes of incubation at 25ºC, the nucleosome acidic patch antibody, PL2-6 (116) was added to the mixture and incubated on ice for 10 minutes. The samples were then analyzed by 5-12% gradient non-denaturing PAGE (FUJIFILM Wako Pure Chemical Corporation) followed by EtBr staining.

2.9 Pull-down assay for p53 binding to the histone complex

To validate histone binding by p53, 2.5 μM of the purified H3-H4 complex was mixed with 2.5 μM of either GST, GST-tagged p53, or GST-tagged p53 mutants in buffer 12. After 30 minutes of incubation at 25ºC, the reaction mixture was mixed with 15 μL of GS4B beads (Cytiva) in buffer 13. After 30 minutes of rotation, the beads were collected by centrifugation and washed three times with 1 ml of buffer 14. The proteins co-pelleted with beads were eluted by adding buffer 15 and were heated at 95ºC for 15 minutes. The samples were then electrophoresed by 18% SDS-PAGE, and the protein bands were visualized by CBB staining.

2.10 EMSA for p53 binding to the histone complex

The histone binding by untagged p53 was evaluated by the similar method previously described (117). At first, 15 μM of the H3-H4 complex was mixed with either 0, 3, 6, 9, 12, 15, or 18 μM of p53 or p53 mutants in buffer 16. The mixture was incubated at 25°C for 30 minutes and was then electrophoresed on the non-denaturing 5% PAGE. The p53 binding was visualized CBB staining.

2.11 Preparation of the p53-nucleosome complex

The p53-nucleosome complex for cryo-EM analysis was prepared by gradient fixation method (GraFix) (118). First, the 169 bp nucleosome^{BS} (10 μM) was mixed with the recombinant p53 (40 μM) and incubated at 25 ºC for 30 min in buffer 17. The sample was then carefully applied on the top of a 5-20% (w/v) sucrose gradient solution containing 10 mM HEPES-KOH pH 7.5, 20 mM NaCl, and 2 mM DTT, with increasing concentration (0-2% w/v) of paraformaldehyde (Electron Microscopy Sciences) made by GRADIENT MASTER (BioComp). The Ultra-Clear^{TM} centrifuge tube (Beckman Coulter) was subjected to ultracentrifugation (Beckman SW41Ti rotor, 27000 rpm, 16 hr., 4ºC). Then, the samples were collected from the top of the gradient solution into each fraction tube. The fractions were analyzed by non-denaturing PAGE stained with EtBr. The peak fractions were applied to the PD-10 column (Cytiva) to replace the solvent with buffer 18. Finally, the sample was concentrated with an Amicon Ultra-2 centrifugal filter unit (MWCO 30 kDa) (Millipore). The concentration was determined by DNA concentration at Abs_{260}.

2.12 Cryo-EM data collection

For the cryo-EM specimen preparation, 2.5 μL aliquots of the p53-nucleosome complex were applied to Quantifoil R1.2/1.3 200 mesh copper grids, which were quenched by ethyl acetate and glow-discharged by soft plasma ion bombardment (PIB-10, Vacuum Device Inc.) beforehand. The grids were then blotted and plunged into liquid ethane using Vitrobot Mark IV (Thermo Fisher Scientific). The major parameters for the blotting condition were summarized in Table 4.

The prepared grids were screened and the 8378 frames were then collected automatically with SerialEM (119) with a pixel size of 1.06 Å on Titan Krios G4 (Thermo Fisher Scientific) operated at 300 kV. The digital micrographs were recorded on a K3 BioQuantum (Gatan) direct electron detector in the electron counting mode, using a slit width of 25 eV, and retaining 40 frames with a total dose of ~60 electron/$Å^2$.

2.13 Image processing

Following image processing was performed on RELION3.1 software (120). All movie frames were aligned and dose-weighted using MOTIONCOR2 (121). The CTF estimation was performed by CTFFIND4 (122) from the digital micrographs. The particles were automatically picked with a box size of 280 × 280 pixels. Contaminated junk particles were removed through the process of 2D classification and 3D classification.

The 3D classification processes for the p53-nucleosome complex were performed, followed by particle polishing and a few rounds of CTF refinement. The resolution of the refined 3D map was at 3.9 Å, as estimated by the gold standard FSC

(123). The local resolution map and the angular distribution of the p53-nucleosome complex were calculated by RELION3.1. The details of the processing statistics are listed in Table 5.

2.14 Model building

The cryo-EM structure of the nucleosome (PDB ID: 7OHC) (124) and the crystal structure of the p53-DNA complex (PDB ID: 3KMD) (108) were placed in the cryo-EM map of the p53-nucleosome complex by rigid-body fitting in UCSF Chimera (125). The 20 bp of the nucleosomal DNA edge was then removed and the DNA model generated by Pymol was automatically fitted into the vacant cryo-EM density using ISOLDE (126) on UCSF ChimeraX (127). Finally, the DNA edges were connected and the final model for the p53-nucleosome complex was built with COOT (128, 129).

2.15 Hydroxyl-radical footprinting assay

The 169 bp of fluorescent-labeled DNA fragments were prepared by the PCR method using the commercially obtained 5'-Cy5 labeled DNA primer and 5'-6FAM labeled DNA primer. The nucleosomes for hydroxyl-radical footprinting assay were then reconstituted and purified by the method described in chapter 2.4. The p53 truncated mutants p53DBD (94-293 amino acid residues) and p53CTR (294-393 amino acid residues) were purified by the same method described in chapter 2.1.

For the hydroxyl-radical footprinting experiments (130–132), 0.6 μM of the fluorescent-labeled nucleosomes were mixed with either 2.4 μM of p53, 3.6 μM of

p53DBD, or 3.6 μM of p53CTR in 50 μL of buffer 19 and incubated at 25ºC for 30 minutes. The buffer exchange into buffer 20 was performed by four consecutive filtrations and dilutions using Amicon Ultra-0.5 centrifugal filter units (MWCO 30 kDa). For the hydroxyl radical reaction, 2.5 μL aliquots of 4 mM $FeAmSO_4$/8 mM EDTA, 0.1 M sodium ascorbate, and 0.6% v/v H_2O_2 were separately placed on the cap of the tubes, in which the 50 μl of the quenched sample was at the bottom. The tubes were centrifuged to initiate the reaction by mixing these reagents simultaneously and were incubated for 2 min at room temperature. To terminate the reactions, 5 μl aliquot of 100 mM thiourea and 10 μl aliquot of 3 M sodium acetate (pH 5.2), were added by centrifugation. Finally, the proteinase solution containing 50% v/v ProK and 5% SDS, was mixed and the DNAs were extracted by PCI followed by ethanol precipitation. The DNA samples were denatured by highly deionized formamide (Thermo Fisher Scientific) and fractionated by Urea-PAGE. The fluorescence signals: Cy5 and 6FAM, were detected on the Amersham Typhoon scanner (Cytiva) respectively. The gel images were analyzed using ImageJ software (133).

Chapter 3 Results and discussion

3.1 Biochemical analysis of the p53 binding to the nucleosome

3.1.1 Purification of the recombinant human p53

The recombinant human p53 was overexpressed in the *Escherichia coli* cells and purified by combining GST affinity chromatography, heparin column chromatography, and size exclusion chromatography as described in 2.1. In good agreement with the dimerization nature of p53, the chromatogram peaks followed by SDS-PAGE analysis showed a bi-disperse state of the recombinant p53 (Figure 3-1 A, B). The purity of the final product was validated by SDS-PAGE (Figure 3-1 C). The final yield was about 1 mg per 16 L of LB medium culture.

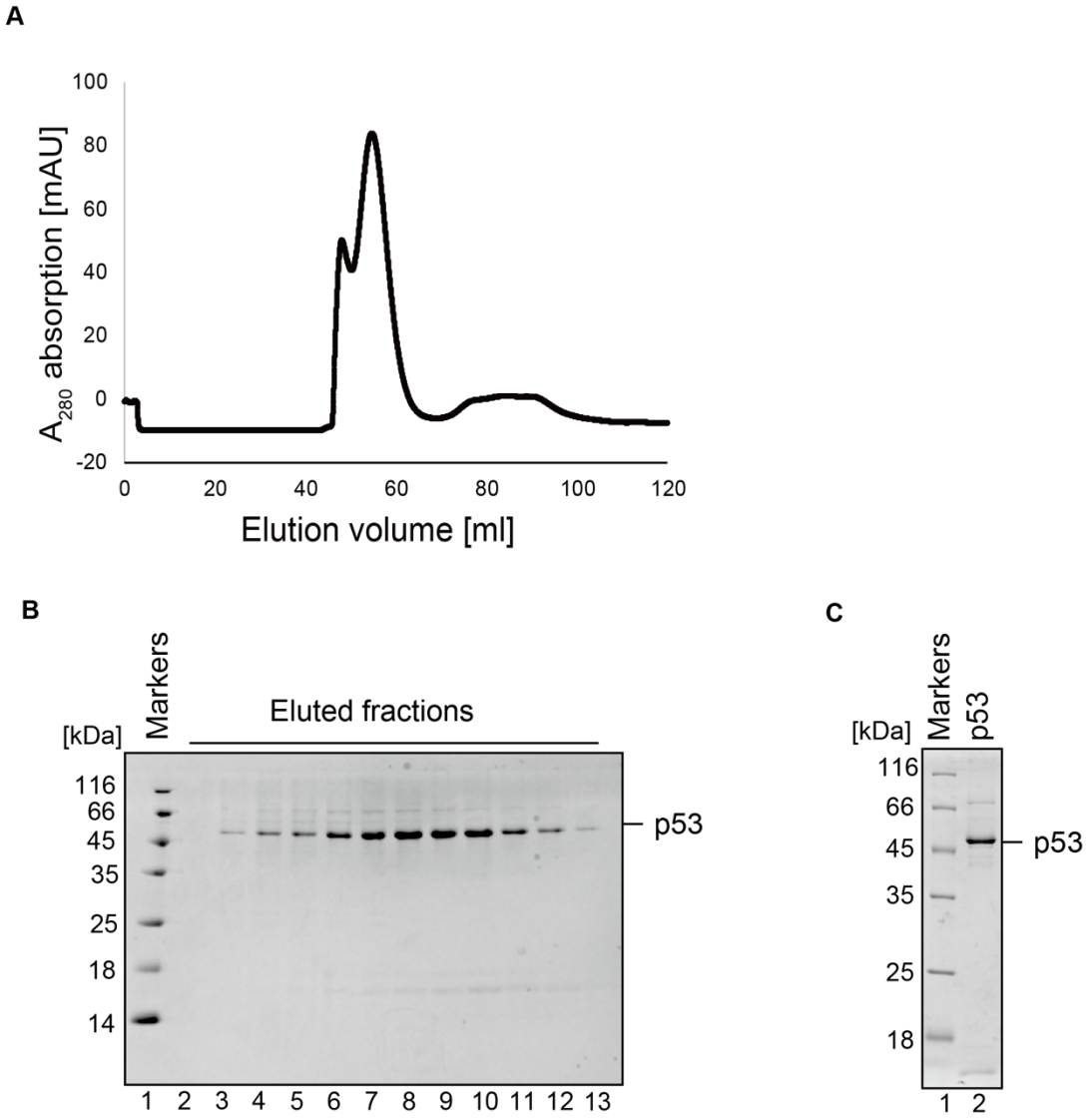

Figure 3-1 Purification of the human p53

(A) Size exclusion chromatogram of the recombinant p53.

(B) SDS-PAGE analysis of the chromatogram peak. Lane 1 indicates protein markers. Lane 2-13 represents eluted fractions. The polyacrylamide gel was stained by CBB.

(C) SDS-PAGE analysis of the purified p53 protein. Lane 1 indicates protein markers, and lane 2 indicates the purified p53. The polyacrylamide gel was stained by CBB.

3.1.2 Purification of the nucleosomes

The histone octamer and DNA fragments were purified as described in 2.2 and 2.3 respectively. To test the nucleosome binding capability of p53 as well as the linker DNA requirement, the minimal 145 bp nucleosome and the 193 bp nucleosome which has 24 bp of linker DNAs were prepared as described in 2.4 (Figure 3-2 A). The purity of the final products was validated by non-denaturing PAGE and SDS-PAGE (Figure 3-2 B, C). In the non-denaturing PAGE, both nucleosomes appeared as major bands above each of the component DNAs. In the SDS-PAGE, both nucleosomes contained equal amounts of four core histones. Together, these gel analyses indicated that the nucleosomes were appropriately reconstituted with high purity.

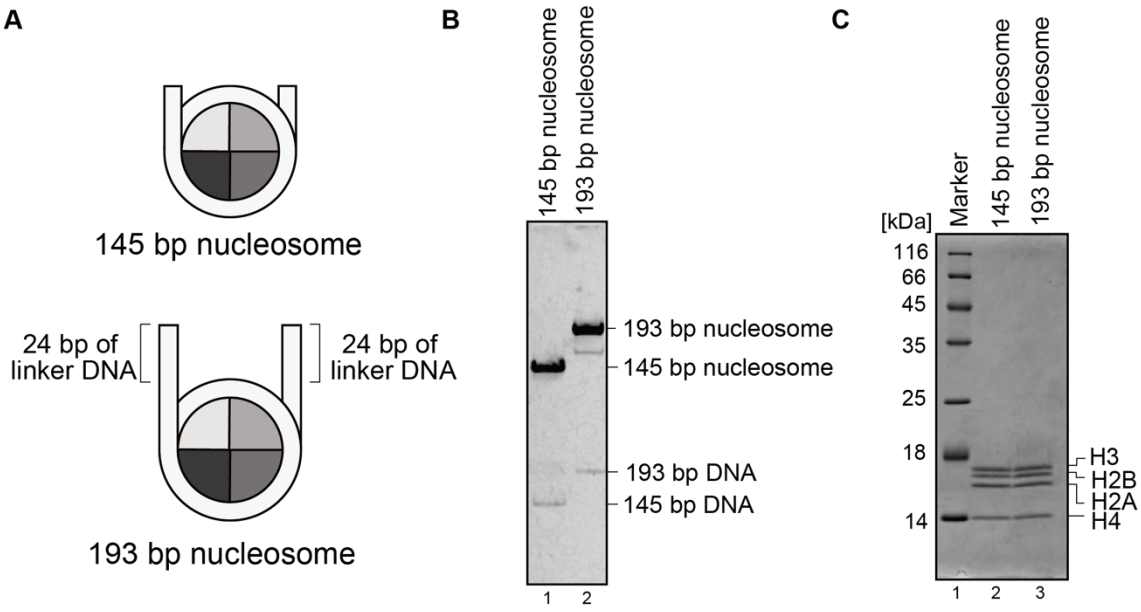

Figure 3-2 Purification of the nucleosomes with or without linker DNAs

(A) Illustration of the nucleosomes. The nucleosome containing 145 bp DNA (145 bp nucleosome, top) and the nucleosome containing 193 bp DNA (193 bp nucleosome, bottom) are illustrated. The 24 bp of linker DNAs on the 193 bp nucleosome edges are indicated.

(B) Native PAGE analysis of the nucleosomes. Lanes 1 and 2 represent the 145 bp nucleosome and the 193 bp nucleosome, respectively. The polyacrylamide gel was stained by EtBr.

(C) SDS-PAGE analysis of the nucleosomes. Lane 1 indicates protein markers. Lanes 2 and 3 represent the 145 bp nucleosome and the 193 bp nucleosome, respectively. The polyacrylamide gel was stained by CBB.

3.1.3 Linker DNAs are required for the p53-nucleosome complex formations

The nucleosome binding capability of p53 was tested by the EMSA as described in 2.5. As seen in Figure 3-3 A, a band corresponding to the 193 bp nucleosome completely shifted when p53 was added 8-fold much molar ratio and formed specific complexes, visualized as four discrete bands on the non-denaturing polyacrylamide gel (Figure 3-3, A, lane 10). In contrast, p53 hardly formed such complexes with the 145 bp nucleosome (Figure 3-3 A, lanes 1-5). Therefore, linker DNA portions in the nucleosome may facilitate specific p53 binding, even without its target DNA sequence. The protein component of the four shifted bands was analyzed by the subsequent 2D protein gel analysis as described in 2.6. In this experiment, the 193 bp nucleosome bound by p53 was first electrophoresed by non-denaturing polyacrylamide gel, after that the gel was analyzed by SDS-PAGE. As a result, the four shifted bands contained four core histones together with p53, indicating that they all represent the p53-nucleosome complexes (Figure 3-3 B). Collectively, these results suggested that p53 specifically binds to the nucleosome via linker DNA portions, in a sequence-nonspecific manner. Because p53 has a tetramerization domain, the four bands are supposed to reflect oligomeric states of p53 bound to the 193 bp nucleosome.

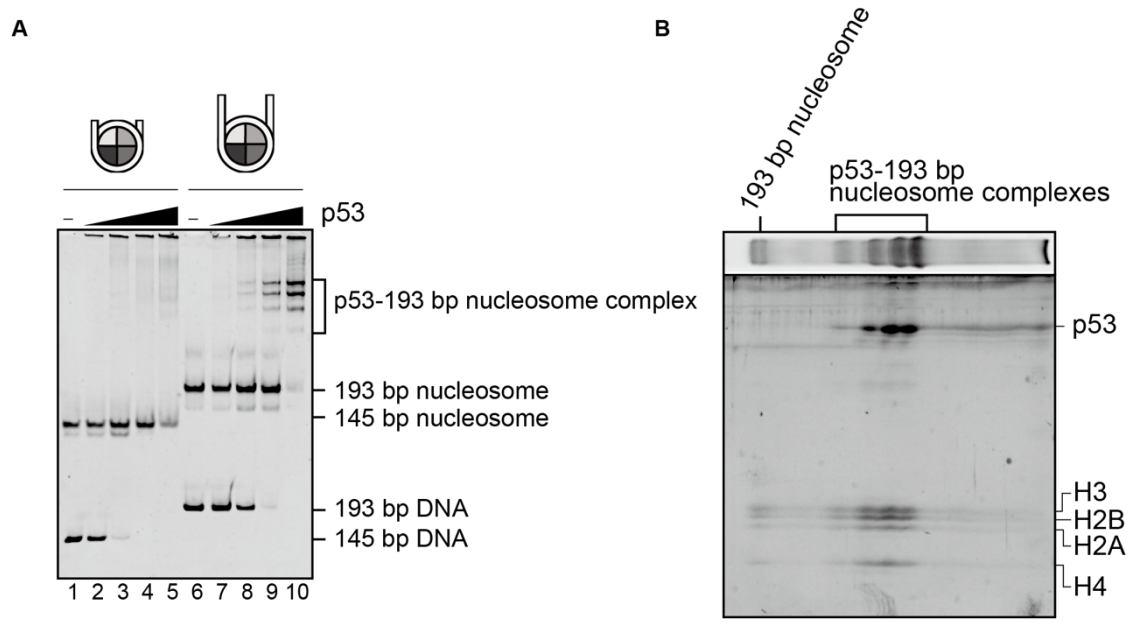

Figure 3-3 p53 binding to the nucleosomes containing linker DNAs

(A) EMSA for p53 binding to the 145 bp nucleosome (lanes 1-5) and the 193 bp nucleosome (lanes 6-10). The nucleosomes were mixed with the increasing molar ratio (0-8 times) of p53. The non-denaturing polyacrylamide gel was stained by EtBr.

(B) 2D protein gel analysis of the p53-193 bp nucleosome complexes. The p53-193 bp nucleosome complexes were first fractionated on a 5-12% gradient gel, followed by EtBr staining (upper). The sample was then denatured in the non-denaturing gel, and analyzed by the SDS-PAGE, followed by CBB staining (lower).

3.1.4 p53 prefers nucleosomal linker DNAs rather than free DNA

To compare the p53 binding affinity of the nucleosome with the histone-free DNA, the competitive binding assay was performed as described in 2.7. As a competitor DNA, the 24 bp of DNA containing the identical sequence with the linker DNA portion of the 193 bp nucleosome was prepared by the method described in 2.3. In this experiment, p53 dissociation from the p53-nucleosome complexes was tested through the nucleosome band appearance on the non-denaturing PAGE. As a result, the p53-nucleosome complexes remained intact even in the presence of a 16-fold amount of the competitor DNA (Figure 3-4, lane 6). This result supports that p53 recognizes the nucleosome structure mediated by the linker DNA even without the target sequence.

The DNA sequence-nonspecific binding to the nucleosomes is consistent with the previously reported FRAP analysis, which observed the slow diffusion rate of p53 in the nucleus (134). A series of the single-molecule analysis suggested that the non-specific DNA binding of p53 facilitates its target sequence searching on the DNA curtain (95–98). Since the natural p53 binding sites are incorporated into nucleosomes (99, 101, 111), the ability of p53 to bind to linker DNA may be important for efficient target sequence search in the context of chromatin environment. Such sequence-nonspecific nucleosome binding ability is also known for other pioneer transcription factors, such as FoxA1, and may be required for recognizing target DNA in closed chromatin regions.

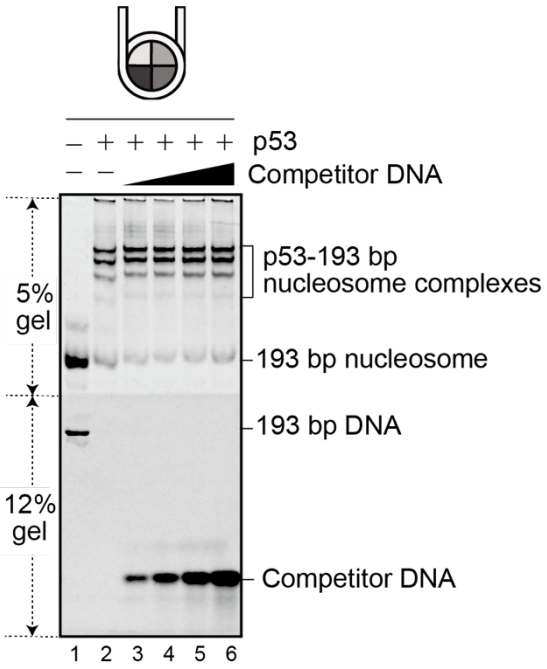

Figure 3-4 Competitive nucleosome-binding assay for p53

Lanes 1 and 2 indicate the 193 bp nucleosome and the p53-193 bp nucleosome complex, respectively. Lanes 3 to 6 indicate the p53-nucleosome complexes mixed with the increasing molar ratio (1-16 times) of competitor DNA. The non-denaturing biphasic polyacrylamide gel (upper gel (5%) and lower gel (12%)) was stained by EtBr.

3.1.5 p53 can readout the target DNA sequence within the nucleosomal edge

To examine how the p53 binding sequence affects the formation of the p53-nucleosome complexes, the 193 bp nucleosome containing p53 binding sequence (193 bp nucleosome^{BS}) was prepared as the way described in 2.5. Since natural target sites of p53 reside around the nucleosomal edge (SHL(±7)) *in vivo* (100, 111), the 193 bp nucleosome^{BS} was constructed to contain 20 bp of optimized p53 binding sequence between SHL(6) and SHL(8) to mimic the p53 target nucleosome (Figure 3-5 A). The non-denaturing PAGE and SDS-PAGE analysis showed that the prepared 193 bp nucleosome^{BS} was highly purified (Figure 3-5 B, C). The EMSA using the 193 bp nucleosome and the 193 bp nucleosome^{BS} showed that p53 efficiently bound to both nucleosomes as seen by their band disappearance. Notably, p53 formed an additional specific complex with the 193 bp nucleosome^{BS}, that appeared as an additional band on the polyacrylamide gel (Figure 3-5 D, red arrow). Subsequent EMSA using a nucleosome-specific antibody, PL2-6 (116), confirmed that the additional specific band contains the nucleosome (Figure 3-5 E, lanes 3 and 4, red arrow). Together, these results suggest that p53 can recognize the p53 binding sequence inserted between SHL(6) and SHL(8) of the nucleosome.

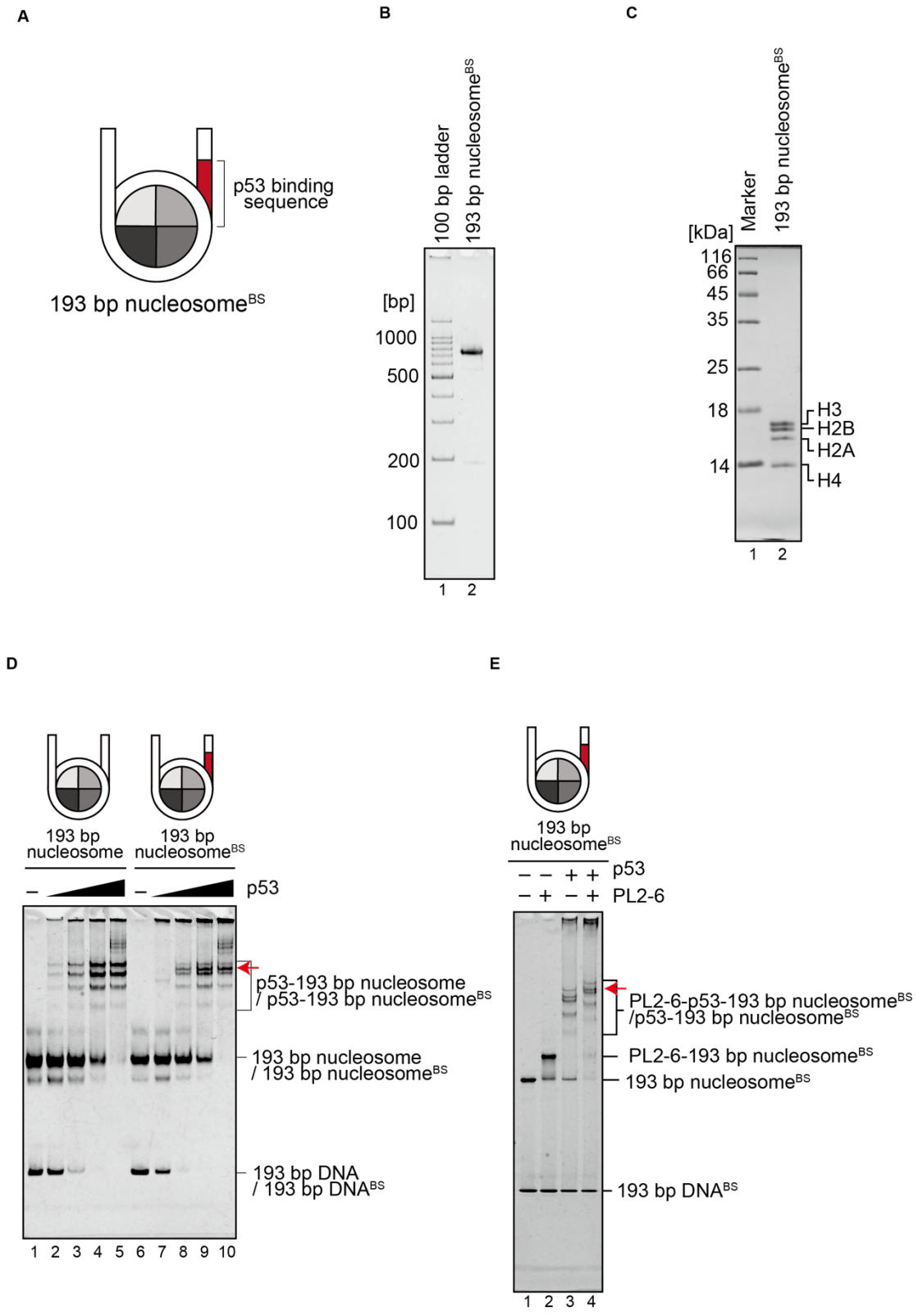
A
p53 binding sequence
193 bp nucleosome^BS
B
100 bp ladder
193 bp nucleosome^BS
[bp]
1000
500
200
100
1 2
C
[kDa]
Marker
193 bp nucleosome^BS
116
66
45
35
25
18
14
H3
H2B
H2A
H4
1 2
D
193 bp nucleosome
193 bp nucleosome^BS
–
p53
p53-193 bp nucleosome / p53-193 bp nucleosome^BS
193 bp nucleosome / 193 bp nucleosome^BS
193 bp DNA / 193 bp DNA^BS
1 2 3 4 5 6 7 8 9 10
E
193 bp nucleosome^BS
– – + + p53
– + – + PL2-6
PL2-6-p53-193 bp nucleosome^BS /p53-193 bp nucleosome^BS
PL2-6-193 bp nucleosome^BS
193 bp nucleosome^BS
193 bp DNA^BS
1 2 3 4

Figure 3-5 p53 binding to the nucleosomes containing a target DNA sequence

(A) Illustration of the 193 bp nucleosome^{BS}, in which the 20 bp of p53 binding sequence was inserted between SHL(6) to SHL(8) of the nucleosomal DNA. The p53 binding sequence is colored in red.

(B) Native PAGE analysis of the 193 bp nucleosome^{BS}. Lane 1 indicates the bp ladder, and lane 2 indicates the 193 bp nucleosome^{BS}. The non-denaturing polyacrylamide gel was stained by EtBr.

(C) SDS-PAGE analysis of the 193 bp nucleosome^{BS}. Lane 1 indicates protein markers, and lane 2 indicates the 193 bp nucleosome^{BS}. The polyacrylamide gel was stained by CBB.

(D) EMSA for p53 binding to the 193 bp nucleosomes (lanes 1-5) and the 193 bp nucleosome^{BS} (lanes 6-10). The nucleosomes were mixed with the increasing molar ratio (0-8 times) of p53. The non-denaturing polyacrylamide gel was stained by EtBr. A red arrow indicates the specific band representing the sequence-specific binding to the nucleosome of p53.

(E) EMSA for PL2-6 binding to the p53-nucleosome complexes. Lanes 1 and 2 indicate the 193 bp nucleosome^{BS} without/with PL2-6, respectively. Lanes 3 and 4 indicate the p53-193 bp nucleosome^{BS} complexes without/with PL2-6, respectively. The non-denaturing polyacrylamide gel was stained by EtBr. The band shift of the specific complex is indicated by a red arrow.

3.1.6 N-terminal amino acid region of p53 directly interacts with the H3-H4 complex

In the structure of the nucleosome, the H3-H4 complex is placed on the dyad region and interacts with the nucleosomal entry/exit site DNAs (Figure 1-1 C), thereby p53 binding ability to the H3-H4 complex was tested employing the GST pull-down experiment. To do so, p53 and its truncation mutants containing either the 1-93 amino acid region (p53NTR) or the 94-393 amino acid region (p53ΔNTR) were prepared as GST-tagged proteins as described in 2.1 (Figure 3-6 A and Figure 3-6 B, lanes 3-5). In the pull-down experiment, the purified H3-H4 complex was mixed with each of GST-tagged p53 and GST-tagged p53 mutants, and the binding capability was evaluated by the H3-H4 complex co-precipitation with GS4B beads as described in 2.9. As a result, the H3-H4 complex co-precipitated with p53FL and p53NTR, but not with p53ΔNTR (Figure 3-6 B). This result is also confirmed with the protein EMSA performed as described in 2.10. The protein bands corresponding to the H3-H4 complex on the polyacrylamide gel was gradually disappeared by adding the un-tagged p53FL and p53NTR while adding p53ΔNTR did not interfere with (Figure 3-6 C). Together, these results indicate the direct interaction between the histone H3-H4 complex and the N-terminal amino acid region of p53.

The p53 N-terminal region contains TAD1 and TAD2 (87, 135) (Figure 3-6 A), which are required for p53 target gene induction (136). These domains are known to bind to various factors including general transcription factors, mediators, and transcriptional coactivators such as CBP/p300 (137, 138), implying that the p53 N-terminal amino acid region may function as an interaction hub for transcription co-factors and histones (90, 139). Histone binding ability is also known for another

pioneer factor: FoxA1 (140), thereby it may be a common property of pioneer transcription factors.

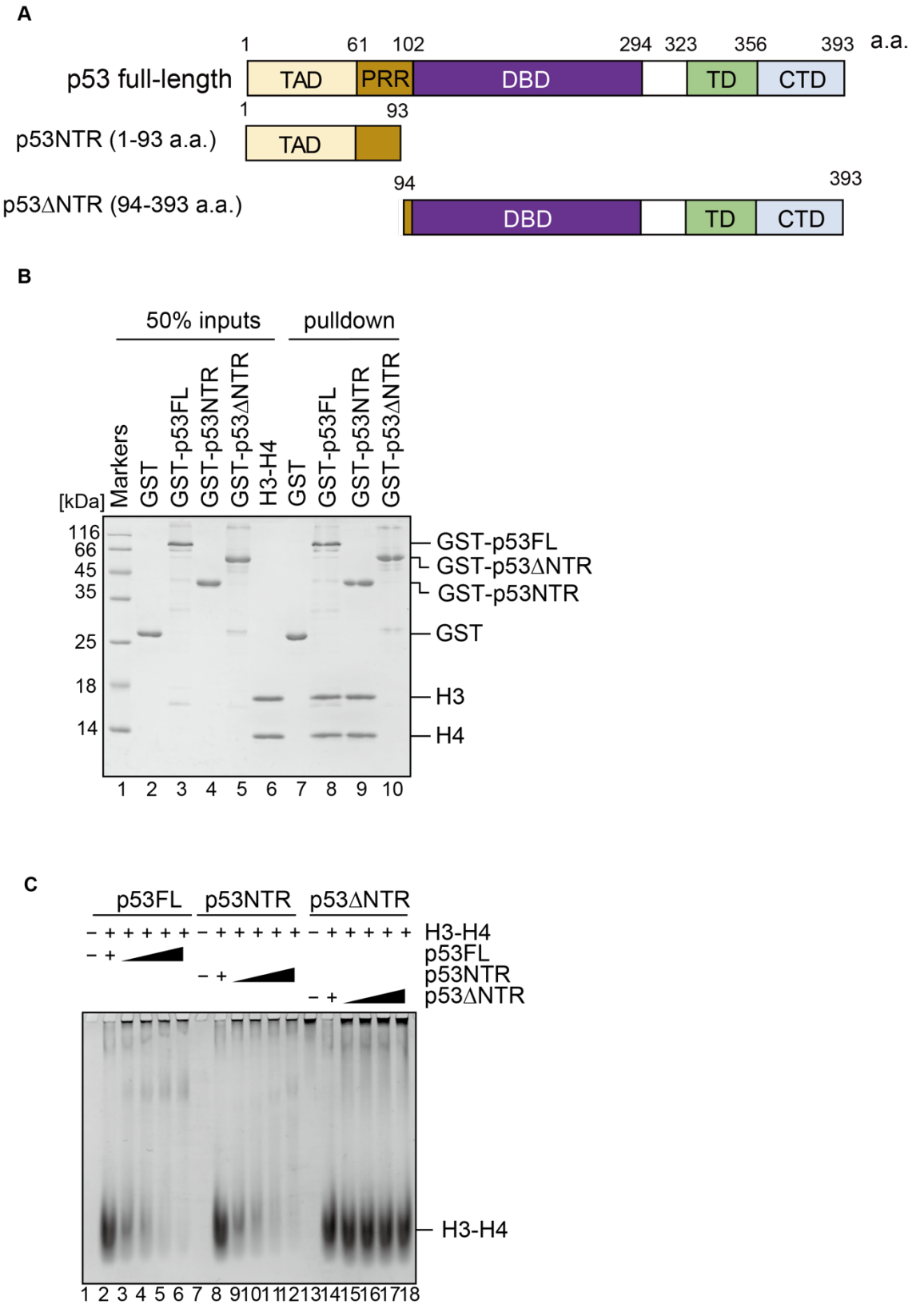
A
p53 full-length
TAD
PRR
DBD
TD
CTD
1
61
102
294
323
356
393
a.a.
p53NTR (1-93 a.a.)
93
p53ΔNTR (94-393 a.a.)
94
B
50% inputs
pulldown
Markers
GST
GST-p53FL
GST-p53NTR
GST-p53ΔNTR
H3-H4
[kDa]
116
66
45
35
25
18
14
GST-p53FL
GST-p53ΔNTR
GST-p53NTR
GST
H3
H4
1 2 3 4 5 6 7 8 9 10
C
p53FL
p53NTR
p53ΔNTR
H3-H4
H3-H4
1 2 3 4 5 6 7 8 9 10 11 12 13 14 15 16 17 18

Figure 3-6 p53 binding to the histone H3-H4 complex

(A) Schematic representation of p53 and p53 truncation mutants. The p53 full-length (p53FL), the truncation mutant containing 1-93 amino acid residues (p53NTR), and the truncation mutant containing 94-393 amino acid residues (p53ΔNTR) are shown. Within these constructs, transcription activation domains (TAD), proline-rich region (PRR), core DNA-binding domain (DBD), tetramerization domain (TD), and C-terminus domain (CTD) are colored in beige, khaki, indigo, cobalt green, and sky blue, respectively.

(B) Pull-down assay for p53 binding to the histone H3-H4 complex. Lane 1 indicates protein markers. Lanes 2-6 represent the control samples of GST, GST-p53FL, GST-p53NTD, GST-p53ΔN, and the H3-H4 complex, respectively. Lanes 7-10 indicate the pull-down experiment for the histone H3-H4 complex binding with GST, GST-p53FL, GST-p53NTD, and GST-p53ΔNTR, respectively. The polyacrylamide gel was stained by CBB.

(C) Protein EMSA for histone binding. The H3-H4 complex was mixed with the increasing molar ratio (0.6-1.2 times) of either untagged p53FL (lanes 2-6), p53NTR (lanes 8-12), or p53ΔNTR (lanes 13-18). The non-denaturing polyacrylamide gel was stained by CBB.

3.1.7 N-terminal amino acid region of p53 may involve the nucleosome bindings

To test whether the histone H3-H4 binding via N-terminal amino acid region of p53 involves its nucleosome binding, EMSA using p53ΔNTR, 193 bp nucleosome, and 193 bp nucleosome^{BS} was performed as described in 2.5. As a result, the p53ΔNTR-nucleosome complexes were seen as faint bands on the polyacrylamide gel compared to the p53-nucleosome complexes (Figure 3-7). This result suggests that the p53-histone interaction mediated by the N-terminal amino acid region facilitates the formations of p53-nucleosome complexes in a sequence-nonspecific manner.

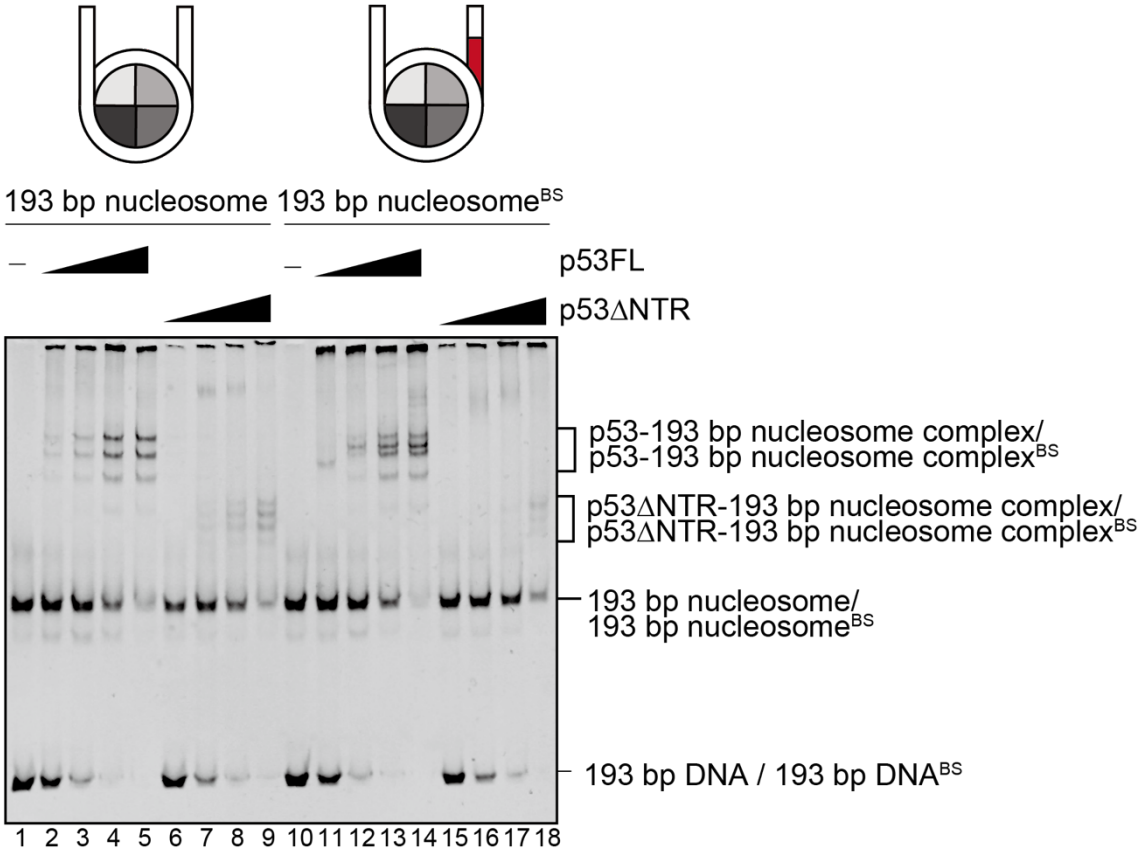

Figure 3-7 p53ΔNTR bindings to the nucleosomes

EMSA for p53ΔNTR binding to the nucleosomes. The 193 bp nucleosome or the 193 bp nucleosome^{BS} were mixed with the increasing molar ratio (0-8 times) of p53 (lanes 1-5 and 10-14) or p53ΔNTR (lanes 6-9 and 15-18). The non-denaturing polyacrylamide gel was stained by EtBr.

第 3 章 2 項については、5 年以内に雑誌などで刊行予定のため、

非公開

Chapter 4: Concluding remarks and future perspectives

4.1 Biochemical properties of the pioneer transcription factor p53 binding to the nucleosomes

The pioneer transcription factor p53 can bind to the target DNA within a nucleosome, which is inaccessible to most of the transcription factors. In this study, p53 was found to bind to nucleosomes via linker DNAs even without its binding sequence. The sequence non-specific nucleosome binding is also known in other pioneer transcription factors including FoxA1 (134, 142–144). But the binding mode of FoxA1 does not require the linker DNAs (143) therefore, the non-specific nucleosome binding mechanisms are supposed to vary among pioneer transcription factors. In addition to DNA bindings, p53 interacted with the histone H3-H4 complex via its N-terminal amino acid region. Functional studies have revealed that TAD1 and TAD2 within the N-terminal amino acid region of p53 are required for the target genes induction (136). Similarly, a pioneer transcription factor FoxA1 can also bind the histone H3-H4 complex via its C-terminal domain, which is separated from its DNA-binding domain and such interaction is necessary for the chromatin opening (66, 140). Besides, another pioneer transcription factor EBF1 is also reported to engage its C-terminal domain for chromatin opening during B-cell development (145). It has been speculative yet, but the sequence-nonspecific nucleosome binding and the histone binding would be common properties of pioneer transcription factors that enable the target DNA searching embedded in closed chromatin and the transcriptional co-factors engagement. Further studies are expected to dissect the mechanistic link between histone binding and pioneering activities.

第 4 章 2 項については、5 年以内に雑誌などで刊行予定のため、

非公開

Reference

1. Koonin, E. V., and Wolf, Y.I. (2008) Genomics of bacteria and archaea: The emerging dynamic view of the prokaryotic world. *Nucleic Acids Res.*, 36, 6688–6719.

2. Koonin, E. V. (2009) Evolution of genome architecture. *Int. J. Biochem. Cell Biol.*, 41, 298–306.

3. Alberts, B., Bray, D., Hopkins, K., Johnson, A., Lewis, J., Raff, M., Roberts, K., and Walter, P. (2009) Essential Cell Biology, 3rd edition.

4. Paweletz, N. (2001) Walther Flemming: Pioneer of mitosis research. *Nat. Rev. Mol. Cell Biol.*, 2, 72–75.

5. Olins, A.L., and Olins, D.E. (1974) Spheroid chromatin units (v bodies). *Science*, 183, 330–332.

6. Woodcock, C.L.F., Safer, J.P., and Stanchfield, J.E. (1976) Structural repeating units in chromatin. *Exp. Cell Res.*, 97, 101–110.

7. Kornberg, D.R. (1974) Chromatin structure: a repeating unit of histones and DNA. *Science*, 184, 868–871.

8. Luger, K., Mäder, A.W., Richmond, R.K., Sargent, D.F., and Richmond, T.J. (1997) Crystal structure of the nucleosome core particle at 2.8 Å resolution. *Nature*, 389, 251–260.

9. Harp, J.M., Hanson, B.L., Timm, D.E., and Bunick, G.J. (2000) Asymmetries in the nucleosome core particle at 2.5 Å resolution. *Acta Crystallogr. Sect. D Biol. Crystallogr.*, 56, 1513–1534.

10. Davey, C.A., Sargent, D.F., Luger, K., Maeder, A.W., and Richmond, T.J. (2002) Solvent mediated interactions in the structure of the nucleosome core particle at 1.9 Å resolution. *J. Mol. Biol.*, 319, 1097–1113.

11. Richmond, T.J., and Davey, C.A. (2003) The structure of DNA in the nucleosome core. *Nature*, 423, 145–150.

12. Tan, S., and Davey, C.A. (2011) Nucleosome structural studies. *Curr. Opin. Struct. Biol.*, 21, 128–136.

13. Tsunaka, Y., Kajimura, N., Tate, S.I., and Morikawa, K. (2005) Alteration of the nucleosomal DNA path in the crystal structure of a human nucleosome core particle. *Nucleic Acids Res.*, 33, 3424–3434.

14. Ueda, J., Harada, A., Urahama, T., Machida, S., Maehara, K., Hada, M., Makino, Y., Nogami, J., Horikoshi, N., Osakabe, A., *et al.* (2017) Testis-Specific Histone Variant H3t Gene Is Essential for Entry into Spermatogenesis. *Cell Rep.*, 18, 593–600.

15. Clapier, C.R., Chakravarthy, S., Petosa, C., Fernández-Tornero, C., Luger, K., and Müller, C.W. (2008) Structure of the Drosophila nucleosome core particle highlights evolutionary constraints on the H2A-H2B histone dimer. *Proteins Struct. Funct. Genet.*, 71, 1–7.

16. White, C.L., Suto, R.K., and Luger, K. (2001) Structure of the yeast nucleosome core particle reveals fundamental changes in internucleosome interactions. *EMBO J.*, 20, 5207–5218.

17. Sato, S., Takizawa, Y., Hoshikawa, F., Dacher, M., Tanaka, H., Tachiwana, H., Kujirai, T., Iikura, Y., Ho, C.H., Adachi, N., *et al.* (2021) Cryo-EM structure of the nucleosome core particle containing Giardia lamblia histones. *Nucleic Acids Res.*, 49, 8934–8946.

18. Yuan, G.C., Liu, Y.J., Dion, M.F., Slack, M.D., Wu, L.F., Altschuler, S.J., and Rando, O.J. (2005) Molecular biology: Genome-scale identification of nucleosome positions in S. cerevisiae. *Science*, 309, 626–630.

19. Lee, W., Tillo, D., Bray, N., Morse, R.H., Davis, R.W., Hughes, T.R., and Nislow, C. (2007) A high-resolution atlas of nucleosome occupancy in yeast. *Nat. Genet.*, 39, 1235–1244.

20. Mavrich, T.N., Ioshikhes, I.P., Venters, B.J., Jiang, C., Tomsho, L.P., Qi, J., Schuster, S.C., Albert, I., and Pugh, B.F. (2008) A barrier nucleosome model for statistical positioning of nucleosomes throughout the yeast genome. *Genome Res.*, 18, 1073–1083.

21. Mavrich, T.N., Jiang, C., Ioshikhes, I.P., Li, X., Venters, B.J., Zanton, S.J., Tomsho, L.P., Qi, J., Glaser, R.L., Schuster, S.C., *et al.* (2008) Nucleosome organization in the Drosophila genome. *Nature*, 453, 358–362.

22. Shivaswamy, S., Bhinge, A., Zhao, Y., Jones, S., Hirst, M., and Iyer, V.R. (2008) Dynamic remodeling of individual nucleosomes across a eukaryotic genome in response to transcriptional perturbation. *PLoS Biol.*, 6, 0618–0630.

23. Valouev, A., Ichikawa, J., Tonthat, T., Stuart, J., Ranade, S., Peckham, H., Zeng, K., Malek, J.A., Costa, G., McKernan, K., *et al.* (2008) A high-resolution, nucleosome position map of C. elegans reveals a lack of universal sequence-dictated positioning. *Genome Res.*, 18, 1051–1063.

24. Valouev, A., Johnson, S.M., Boyd, S.D., Smith, C.L., Fire, A.Z., and Sidow, A. (2011) Determinants of nucleosome organization in primary human cells. *Nature*, 474, 516–522.

25. Ye, Y., Wu, H., Chen, K., Clapier, C.R., Verma, N., Zhang, W., Deng, H., Cairns, B.R., Gao, N., and Chen, Z. (2019) Structure of the RSC complex bound to the nucleosome. *Science*, 366, 838–843.

26. He, S., Wu, Z., Tian, Y., Yu, Z., Yu, J., Wang, X., Li, J., Liu, B., and Xu, Y. (2020) Structure of nucleosome-bound human BAF complex. *Science*, 367, 875–881.

27. Wagner, F.R., Dienemann, C., Wang, H., Stützer, A., Tegunov, D., Urlaub, H., and Cramer, P. (2020) Structure of SWI/SNF chromatin remodeller RSC bound to a nucleosome. *Nature*, 579, 448–451.

28. Jin, J., Bai, L., Johnson, D.S., Fulbright, R.M., Kireeva, M.L., Kashlev, M., and Wang, M.D. (2010) Synergistic action of RNA polymerases in overcoming the nucleosomal barrier. *Nat. Struct. Mol. Biol.*, 17, 745–752.

29. Raveh-Sadka, T., Levo, M., Shabi, U., Shany, B., Keren, L., Lotan-Pompan, M., Zeevi, D., Sharon, E., Weinberger, A., and Segal, E. (2012) Manipulating nucleosome disfavoring sequences allows fine-tune regulation of gene expression in yeast. *Nat. Genet.*, 44, 743–750.

30. Teves, S.S., Weber, C.M., and Henikoff, S. (2014) Transcribing through the nucleosome. *Trends Biochem. Sci.*, 39, 577–586.

31. Chen, F.X., Smith, E.R., and Shilatifard, A. (2018) Born to run: Control of transcription elongation by RNA polymerase II. *Nat. Rev. Mol. Cell Biol.*, 19, 464–478.

32. Lorch, Y., LaPointe, J.W., and Kornberg, R.D. (1987) Nucleosomes inhibit the initiation of transcription but allow chain elongation with the displacement of histones. *Cell*, 49, 203–210.

33. Thurman, R.E., Rynes, E., Humbert, R., Vierstra, J., Maurano, M.T., Haugen, E., Sheffield, N.C., Stergachis, A.B., Wang, H., Vernot, B., *et al.* (2012) The accessible chromatin landscape of the human genome. *Nature*, 489, 75–82.

34. Neph, S., Vierstra, J., Stergachis, A.B., Reynolds, A.P., Haugen, E., Vernot, B., Thurman, R.E., John, S., Sandstrom, R., Johnson, A.K., *et al.* (2012) An expansive human regulatory lexicon encoded in transcription factor footprints. *Nature*, 489, 83–90.

35. Zhu, F., Farnung, L., Kaasinen, E., Sahu, B., Yin, Y., Wei, B., Dodonova, S.O., Nitta, K.R., Morgunova, E., Taipale, M., *et al.* (2018) The interaction landscape between transcription factors and the nucleosome. *Nature*, 562, 76–81.

36. Kornberg, R.D., and Lorch, Y. (1999) Twenty-five years of the nucleosome, fundamental particle of the eukaryote chromosome. *Cell*, 98, 285–294.

37. Bai, L., and Morozov, A. V. (2010) Gene regulation by nucleosome positioning. *Trends Genet.*, 26, 476–483.

38. Lai, W.K.M., and Pugh, B.F. (2017) Understanding nucleosome dynamics and their links to gene expression and DNA replication. *Nat. Rev. Mol. Cell Biol.*, 18, 548–562.

39. Workman, J.L., and Kingston, R.E. (1998) Alteration of nucleosome structure as a mechanism of transcriptional regulation. *Annu. Rev. Biochem.*, 67, 545–79.

40. Zhou, K., Gaullier, G., and Luger, K. (2019) Nucleosome structure and dynamics are coming of age. *Nat. Struct. Mol. Biol.*, 26, 3–13.

41. Koyama, M., and Kurumizaka, H. (2018) Structural diversity of the nucleosome. *J. Biochem.*, 163, 85–95.

42. Franklin, S.G., and Zweidler, A. (1977) Non-allelic variants of histones 2a, 2b and 3 in mammals. *Nature*, 266, 273–275.

43. Kurumizaka, H., Kujirai, T., and Takizawa, Y. (2021) Contributions of Histone Variants in Nucleosome Structure and Function. *J. Mol. Biol.*, 433, 166678.

44. Kouzarides, T. (2007) Chromatin Modifications and Their Function. *Cell*, 128, 693–705.

45. Bannister, A.J., and Kouzarides, T. (2011) Regulation of chromatin by histone modifications. *Cell Res.*, 21, 381–395.

46. Anderson, J.D., and Widom, J. (2000) Sequence and position-dependence of the equilibrium accessibility of nucleosomal DNA target sites. *J. Mol. Biol.*, 296, 979–987.

47. Li, G., Levitus, M., Bustamante, C., and Widom, J. (2005) Rapid spontaneous accessibility of nucleosomal DNA. *Nat. Struct. Mol. Biol.*, 12, 46–53.

48. Tims, H.S., Gurunathan, K., Levitus, M., and Widom, J. (2011) Dynamics of nucleosome invasion by DNA binding proteins. *J. Mol. Biol.*, 411, 430–448.

49. Armeev, G.A., Kniazeva, A.S., Komarova, G.A., Kirpichnikov, M.P., and Shaytan, A.K. (2021) Histone dynamics mediate DNA unwrapping and sliding in nucleosomes. *Nat. Commun.*, 12, 2387.

50. Garvie, C.W., and Wolberger, C. (2001) Recognition of specific DNA sequences. *Mol. Cell*, 8, 937–946.

51. Vaquerizas, J.M., Kummerfeld, S.K., Teichmann, S.A., and Luscombe, N.M. (2009) A census of human transcription factors: Function, expression and evolution. *Nat. Rev. Genet.*, 10, 252–263.

52. Lambert, S.A., Jolma, A., Campitelli, L.F., Das, P.K., Yin, Y., Albu, M., Chen, X., Taipale, J., Hughes, T.R., and Weirauch, M.T. (2018) The Human Transcription Factors. *Cell*, 172, 650–665.

53. Damante, G., Fabbro, D., Pellizzari, L., Civitareale, D., Guazzi, S., Polycarpou-schwartz, M., Cauci, S., Quadrifoglio, F., Formisano, S., and Di Lauro, R. (1994) Sequence-specific DNA recognition by the thyroid transcription factor-1 homeodomain. *Nucleic Acids Res.*, 22, 3075–3083.

54. Geertz, M., Shore, D., and Maerkl, S.J. (2012) Massively parallel measurements of molecular interaction kinetics on a microfluidic platform. *Proc. Natl. Acad. Sci. U. S. A.*, 109, 16540–16545.

55. Bejerano, G., Pheasant, M., Makunin, I., Stephen, S., Kent, W.J., Mattick, J.S., and Haussler, D. (2004) Ultraconserved elements in the human genome. *Science*, 304, 1321–1325.

56. Gertz, J., Reddy, T.E., Varley, K.E., Garabedian, M.J., and Myers, R.M. (2012) Genistein and bisphenol A exposure cause estrogen receptor 1 to bind thousands of sites in a cell type-specific manner. *Genome Res.*, 22, 2153–2162.

57. Iwafuchi-Doi, M., and Zaret, K.S. (2014) Pioneer transcription factors in cell reprogramming. *Genes Dev.*, 28, 2679–2692.

58. Zaret, K.S., and Mango, S.E. (2016) Pioneer transcription factors, chromatin dynamics, and cell fate control. *Curr. Opin. Genet. Dev.*, 37, 76–81.

59. Zaret, K.S. (2020) Pioneer Transcription Factors Initiating Gene Network Changes. *Annu. Rev. Genet.*, 54, 367–385.

60. Gualdi, R., Bossard, P., Zheng, M., Hamada, Y., Coleman, J.R., and Zaret, K.S. (1996) Hepatic specification of the gut endoderm in vitro: Cell signaling and transcriptional control. *Genes Dev.*, 10, 1670–1682.

61. Bossard, P., and Zaret, K.S. (1998) GATA transcription factors as potentiators of gut endoderm differentiation. *Development*, 125, 4909–4917.

62. Bossard, P., and Zaret, K.S. (2000) Repressive and restrictive mesodermal interactions with gut endoderm: Possible relation to Meckel's Diverticulum. *Development*, 127, 4915–4923.

63. McPherson, C.E., Shim, E.Y., Friedman, D.S., and Zaret, K.S. (1993) An active tissue-specific enhancer and bound transcription factors existing in a precisely positioned nucleosomal array. *Cell*, 75, 387–398.

64. Shim, E.Y., Woodcock, C., and Zaret, K.S. (1998) Nucleosome positioning by the winged helix transcription factor HNF3. *Genes Dev.*, 12, 5–10.

65. Cirillo, L.A., and Zaret, K.S. (1999) An early developmental transcription factor complex that is more stable on nucleosome core particles than on free DNA. *Mol. Cell*, 4, 961–969.

66. Cirillo, L.A., McPherson, C.E., Bossard, P., Stevens, K., Cherian, S., Shim, E.Y., Clark, K.L., Burley, S.K., and Zaret, K.S. (1998) Binding of the winged-helix transcription factor HNF3 to a linker histone site on the nucleosome. *EMBO J.*, 17, 244–254.

67. Cirillo, L.A., Lin, F.R., Cuesta, I., Friedman, D., Jarnik, M., and Zaret, K.S. (2002) Opening of compacted chromatin by early developmental transcription factors HNF3 (FoxA) and GATA-4. *Mol. Cell*, 9, 279–289.

68. Soufi, A., Donahue, G., and Zaret, K.S. (2012) Facilitators and impediments of the pluripotency reprogramming factors' initial engagement with the genome. *Cell*, 151, 994–1004.

69. Soufi, A., Garcia, M.F., Jaroszewicz, A., Osman, N., Pellegrini, M., and Zaret, K.S. (2015) Pioneer transcription factors target partial DNA motifs on nucleosomes to initiate reprogramming. *Cell*, 161, 555–568.

70. Fernandez Garcia, M., Moore, C.D., Schulz, K.N., Alberto, O., Donague, G., Harrison, M.M., Zhu, H., and Zaret, K.S. (2019) Structural Features of Transcription Factors Associating with Nucleosome Binding. *Mol. Cell*, 75, 921-932.e6.

71. Adachi, K., Kopp, W., Wu, G., Heising, S., Greber, B., Stehling, M., Araúzo-Bravo, M.J., Boerno, S.T., Timmermann, B., Vingron, M., *et al.* (2018) Esrrb Unlocks Silenced Enhancers for Reprogramming to Naive Pluripotency. *Cell Stem Cell*, 23, 266-275.e6.

72. Fiedler, M., Graeb, M., Mieszczanek, J., Rutherford, T.J., Johnson, C.M., and Bienz, M. (2015) An ancient Pygo-dependent Wnt enhanceosome integrated by chip/LDB-SSDP. *Elife*, 4, e09073.

73. Gehrke, A.R., Neverett, E., Luo, Y.J., Brandt, A., Ricci, L., Hulett, R.E., Gompers, A., Graham Ruby, J., Rokhsar, D.S., Reddien, P.W., *et al.* (2019) Acoel genome reveals the regulatory landscape of whole-body regeneration. *Science*, 363, eaau6173.

74. McDaniel, S.L., Gibson, T.J., Schulz, K.N., Fernandez Garcia, M., Nevil, M., Jain, S.U., Lewis, P.W., Zaret, K.S., and Harrison, M.M. (2019) Continued Activity of the Pioneer Factor Zelda Is Required to Drive Zygotic Genome Activation. *Mol. Cell*, 74, 185-195.e4.

75. Oldfield, A.J., Yang, P., Conway, A.E., Cinghu, S., Freudenberg, J.M., Yellaboina, S., and Jothi, R. (2014) Histone-Fold Domain Protein NF-Y Promotes Chromatin Accessibility for Cell Type-Specific Master Transcription Factors. *Mol. Cell*, 55, 708–722.

76. Sun, Y., Nien, C.Y., Chen, K., Liu, H.Y., Johnston, J., Zeitlinger, J., and Rushlow, C. (2015) Zelda overcomes the high intrinsic nucleosome barrier at enhancers during Drosophila zygotic genome activation. *Genome Res.*, 25, 1703–1714.

77. Menet, J.S., Pescatore, S., and Rosbash, M. (2014) CLOCK: BMAL1 is a pioneer-like transcription factor. *Genes Dev.*, 28, 8–13.

78. Lai, X., Verhage, L., Hugouvieux, V., and Zubieta, C. (2018) Pioneer factors in animals and plants—colonizing chromatin for gene regulation. *Molecules*, 23, 1914.

79. Mayran, A., and Drouin, J. (2018) Pioneer transcription factors shape the epigenetic landscape. *J. Biol. Chem.*, 293, 13795–13804.

80. Fornes, O., Castro-Mondragon, J.A., Khan, A., Van Der Lee, R., Zhang, X., Richmond, P.A., Modi, B.P., Correard, S., Gheorghe, M., Baranašić, D., *et al.* (2020) JASPAR 2020: Update of the open-Access database of transcription factor binding profiles. *Nucleic Acids Res.*, 48, D87–D92.

81. Iwafuchi-Doi, M. (2018) The mechanistic basis for chromatin regulation by pioneer transcription factors. *Wiley Interdiscip. Rev. Syst. Biol. Med.*, 11, e1427.

82. Hankey, W., Chen, Z., and Wang, Q. (2020) Shaping chromatin states in prostate cancer by pioneer transcription factors. *Cancer Res.*, 80, 2427–2436.

83. Harris, J., Gouhier, A., and Drouin, J. (2021) Pioneer transcription factors in pituitary development and tumorigenesis. *Eur. J. Endocrinol.*, 184, R1–R15.

84. Sunkel, B.D., and Stanton, B.Z. (2021) Pioneer factors in development and cancer. *iScience*, 24, 103132.

85. Vousden, K.H., and Prives, C. (2009) Blinded by the light: The growing complexity of p53. *Cell*, 137, 413–431.

86. Okorokov, A.L., and Orlova, E. V. (2009) Structural biology of the p53 tumour suppressor. *Curr. Opin. Struct. Biol.*, 19, 197–202.

87. Candau, R., Scolnick, D.M., Darpino, P., Ying, C.Y., Halazonetis, T.D., and Berger, S.L. (1997) Two tandem and independent sub-activation domains in the amino terminus of p53 require the adaptor complex for activity. *Oncogene*, 15, 807–816.

88. Venot, C., Maratrat, M., Sierra, V., Conseiller, E., and Debussche, L. (1999) Definition of a p53 transactivation function-deficient mutant and characterization of two independent p53 transactivation subdomains. *Oncogene*, 18, 2405–2410.

89. Zhu, J., Zhou, W., Jiang, J., and Chen, X. (1998) Identification of a novel p53 functional domain that is necessary for mediating apoptosis. *J. Biol. Chem.*, 273, 13030–13036.

90. Raj, N., and Attardi, L.D. (2017) The transactivation domains of the p53 protein. *Cold Spring Harb. Perspect. Med.*, 7, 1–18.

91. Kandoth, C., McLellan, M.D., Vandin, F., Ye, K., Niu, B., Lu, C., Xie, M., Zhang, Q., McMichael, J.F., Wyczalkowski, M.A., *et al.* (2013) Mutational landscape and significance across 12 major cancer types. *Nature*, 502, 333–339.

92. Tamborero, D., Gonzalez-Perez, A., Perez-Llamas, C., Deu-Pons, J., Kandoth, C., Reimand, J., Lawrence, M.S., Getz, G., Bader, G.D., Ding, L., *et al.* (2013) Comprehensive identification of mutational cancer driver genes across 12 tumor types. *Sci. Rep.*, 3, 1–10.

93. Lawrence, M.S., Stojanov, P., Mermel, C.H., Robinson, J.T., Garraway, L.A., Golub, T.R., Meyerson, M., Gabriel, S.B., Lander, E.S., and Getz, G. (2014) Discovery and saturation analysis of cancer genes across 21 tumour types. *Nature*, 505, 495–501.

94. Foord, O.S., Bhattacharya, P., Reich, Z., and Rotter, V. (1991) A DNA binding domain is contained in the C-terminus of wild type p53 protein. *Nucleic Acids Res.*, 19, 5191–5198.

95. McKinney, K., Mattia, M., Gottifredi, V., and Prives, C. (2004) p53 linear diffusion along DNA requires its C terminus. *Mol. Cell*, 16, 413–424.

96. Tafvizi, A., Huang, F., Leith, J.S., Fersht, A.R., Mirny, L.A., and Van Oijen, A.M. (2008) Tumor suppressor p53 slides on DNA with low friction and high stability. *Biophys. J.*, 95, L01–L03.

97. Kamagata, K., Murata, A., Itoh, Y., and Takahashi, S. (2017) Characterization of facilitated diffusion of tumor suppressor p53 along DNA using single-molecule fluorescence imaging. *J. Photochem. Photobiol. C Photochem. Rev.*, 30, 36–50.

98. Murata, A., Itoh, Y., Mano, E., Kanbayashi, S., Igarashi, C., Takahashi, H., Takahashi, S., and Kamagata, K. (2017) One-dimensional search dynamics of tumor suppressor p53 regulated by a disordered C-terminal domain. *Biophys. J.*, 112, 2301–2314.

99. Nili, E.L., Field, Y., Lubling, Y., Widom, J., Oren, M., and Segal, E. (2010) p53 binds preferentially to genomic regions with high DNA-encoded nucleosome occupancy. *Genome Res.*, 20, 1361–1368.

100. Laptenko, O., Beckerman, R., Freulich, E., and Prives, C. (2011) p53 binding to nucleosomes within the p21 promoter in vivo leads to nucleosome loss and transcriptional activation. *Proc. Natl. Acad. Sci. U. S. A.*, 108, 10385–10390.

101. Sammons, M.A., Zhu, J., Drake, A.M., and Berger, S.L. (2015) TP53 engagement with the genome occurs in distinct local chromatin environments via pioneer factor activity. *Genome Res.*, 25, 179–188.

102. Bao, F., LoVerso, P.R., Fisk, J.N., Zhurkin, V.B., and Cui, F. (2017) p53 binding sites in normal and cancer cells are characterized by distinct chromatin context. *Cell Cycle*, 16, 2073–2085.

103. Gévry, N., Ho, M.C., Laflamme, L., Livingston, D.M., and Gaudreau, L. (2007) p21 transcription is regulated by differential localization of histone H2A.Z. *Genes Dev.*, 21, 1869–1881.

104. Cho, Y., Gorina, S., Jeffrey, P.D., and Pavletich, N.P. (1994) Crystal structure of a p53 tumor suppressor-DNA complex: Understanding tumorigenic mutations. *Science*, 265, 346–355.

105. Malecka, K.A., Ho, W.C., and Ho, W.C. (2009) Crystal structure of a p53 core tetramer bound to DNA. *Oncogene*, 28, 325–333.

106. Kitayner, M., Rozenberg, H., Kessler, N., Rabinovich, D., Shaulov, L., Haran, T.E., and Shakked, Z. (2006) Structural basis of DNA recognition by p53 tetramers. *Mol. Cell*, 22, 741–753.

107. Zhao, K., Chai, X., Johnston, K., Clements, A., and Marmorstein, R. (2001) Crystal Structure of the Mouse p53 Core DNA-binding Domain at 2.7 Å Resolution. *J. Biol. Chem.*, 276, 12120–12127.

108. Chen, Y., Dey, R., and Chen, L. (2010) Crystal Structure of the p53 Core Domain Bound to a Full Consensus Site as a Self-Assembled Tetramer. *Structure*, 18, 246–256.

109. El-Deiry, W.S., Kern, S.E., Pietenpol, J.A., Kinzler, K.W., and Vogelstein, B. (1992) Definition of a consensus binding site for p53. *Nat. Genet.*, 1, 45–49.

110. Funk, W.D., Pak, D.T., Karas, R.H., Wright, W.E., and Shay, J.W. (1992) A transcriptionally active DNA-binding site for human p53 protein complexes. *Mol. Cell. Biol.*, 12, 2866–71.

111. Yu, X., and Buck, M.J. (2019) Defining TP53 pioneering capabilities with competitive nucleosome binding assays. *Genome Res.*, 29, 107–115.

112. Kujirai, T., Arimura, Y., Fujita, R., Horikoshi, N., Machida, S., and Kurumizaka, H. (2018) Methods for preparing nucleosomes containing histone variants. *Methods Mol. Biol.*, 1832, 3–20.

113. Lowary, P.T., and Widom, J. (1998) New DNA sequence rules for high affinity binding to histone octamer and sequence-directed nucleosome positioning. *J. Mol. Biol.*, 276, 19–42.

114. Veprintsev, D.B., and Fersht, A.R. (2008) Algorithm for prediction of tumour suppressor p53 affinity for binding sites in DNA. *Nucleic Acids Res.*, 36, 1589–1598.

115. Luger, K., Rechsteiner, T.J., and Richmond, T.J. (1999) Preparation of nucleosome core particle from recombinant histones. *Methods Enzymol.*, 304, 3–19.

116. Zhou, B.R., Yadav, K.N.S., Borgnia, M., Hong, J., Cao, B., Olins, A.L., Olins, D.E., Bai, Y., and Zhang, P. (2019) Atomic resolution cryo-EM structure of a native-like CENP-A nucleosome aided by an antibody fragment. *Nat. Commun.*, 10, 2301.

117. Osakabe, A., Tachiwana, H., Takaku, M., Hori, T., Obuse, C., Kimura, H., Fukagawa, T., and Kurumizaka, H. (2013) Vertebrate Spt2 is a novel nucleolar histone chaperone that assists in ribosomal DNA transcription. *J. Cell Sci.*, 126, 1323–1332.

118. Kastner, B., Fischer, N., Golas, M.M., Sander, B., Dube, P., Boehringer, D., Hartmuth, K., Deckert, J., Hauer, F., Wolf, E., *et al.* (2008) GraFix: Sample preparation for single-particle electron cryomicroscopy. *Nat. Methods*, 5, 53–55.

119. Mastronarde, D.N. (2005) Automated electron microscope tomography using robust prediction of specimen movements. *J. Struct. Biol.*, 152, 36–51.

120. Zivanov, J., Nakane, T., Forsberg, B.O., Kimanius, D., Hagen, W.J.H., Lindahl, E., and Scheres, S.H.W. (2018) New tools for automated high-resolution cryo-EM structure determination in RELION-3. *Elife*, 7, e42166.

121. Zheng, S.Q., Palovcak, E., Armache, J.-P., Verba, K.A., Cheng, Y., and Agard, D.A. (2017) MotionCor2: anisotropic correction of beam-induced motion for improved cryo-electron microscopy. *Nat. Methods*, 14, 331–332.

122. Rohou, A., and Grigorieff, N. (2015) CTFFIND4: Fast and accurate defocus estimation from electron micrographs. *J. Struct. Biol.*, 192, 216–221.

123. Scheres, S.H.W. (2016) Processing of Structurally Heterogeneous Cryo-EM Data in RELION 1st ed. Elsevier Inc.

124. Wang, H., Xiong, L., and Cramer, P. (2021) Structures and implications of TBP–nucleosome complexes. *Proc. Natl. Acad. Sci. U. S. A.*, 118, e2108859118.

125. Pettersen, E.F., Goddard, T.D., Huang, C.C., Couch, G.S., Greenblatt, D.M., Meng, E.C., and Ferrin, T.E. (2004) UCSF Chimera--a visualization system for exploratory research and analysis. *J. Comput. Chem.*, 25, 1605–1612.

126. Croll, T.I. (2018) ISOLDE: A physically realistic environment for model building into low-resolution electron-density maps. *Acta Crystallogr. Sect. D Struct. Biol.*, 74, 519–530.

127. Goddard, T.D., Huang, C.C., Meng, E.C., Pettersen, E.F., Couch, G.S., Morris, J.H., and Ferrin, T.E. (2018) UCSF ChimeraX: Meeting modern challenges in visualization and analysis. *Protein Sci.*, 27, 14–25.

128. Emsley, P., and Cowtan, K. (2004) Coot: Model-building tools for molecular graphics. *Acta Crystallogr. Sect. D Biol. Crystallogr.*, 60, 2126–2132.

129. Emsley, P., Lohkamp, B., Scott, W.G., and Cowtan, K. (2010) Features and development of Coot. *Acta Crystallogr. Sect. D Biol. Crystallogr.*, 66, 486–501.

130. Syed, S.H., Goutte-Gattat, D., Becker, N., Meyer, S., Shukla, M.S., Hayes, J.J., Everaers, R., Angelov, D., Bednar, J., and Dimitrov, S. (2010) Single-base resolution mapping of H1-nucleosome interactions and 3D organization of the nucleosome. *Proc. Natl. Acad. Sci. U. S. A.*, 107, 9620–9625.

131. Ranjan, A., Wang, F., Mizuguchi, G., Wei, D., Huang, Y., and Wu, C. (2015) H2A histone-fold and DNA elements in nucleosome activate SWR1-mediated H2A.Z replacement in budding yeast. *Elife*, 4, e06845.

132. Kujirai, T., Horikoshi, N., Sato, K., Maehara, K., Machida, S., Osakabe, A., Kimura, H., Ohkawa, Y., and Kurumizaka, H. (2016) Structure and function of human histone H3.Y nucleosome. *Nucleic Acids Res.*, 44, 6127–6141.

133. Schneider, C.A., Rasband, W.S., and Eliceiri, K.W. (2012) NIH Image to ImageJ: 25 years of image analysis. *Nat. Methods*, 9, 671–675.

134. Hinow, P., Rogers, C.E., Barbieri, C.E., Pietenpol, J.A., Kenworthy, A.K., and DiBenedetto, E. (2006) The DNA binding activity of p53 displays reaction-diffusion kinetics. *Biophys. J.*, 91, 330–342.

135. Chang, J., Kim, D.-H., Lee, S.W., Kwan, Y.C., and Young, C.S. (1995) Transactivation ability of p53 transcriptional activation domain is directly related

to the binding affinity to TATA-binding protein. *J. Biol. Chem.*, 270, 25014–25019.

136. Brady, C.A., Jiang, D., Mello, S.S., Johnson, T.M., Jarvis, L.A., Kozak, M.M., Broz, D.K., Basak, S., Park, E.J., McLaughlin, M.E., *et al.* (2011) Distinct p53 transcriptional programs dictate acute DNA-damage responses and tumor suppression. *Cell*, 145, 571–583.

137. Teufel, D.P., Freund, S.M., Bycroft, M., and Fersht, A.R. (2007) Four domains of p300 each bind tightly to a sequence spanning both transactivation subdomains of p53. *Proc. Natl. Acad. Sci. U. S. A.*, 104, 7009–7014.

138. Jenkins, L.M.M., Yamaguchi, H., Hayashi, R., Cherry, S., Tropea, J.E., Miller, M., Wlodawer, A., Appella, E., and Mazur, S.J. (2009) Two distinct motifs within the p53 transactivation domain bind to the taz2 domain of p300 and are differentially affected by phosphorylation. *Biochemistry*, 48, 1244–1255.

139. Kaustov, L., Yi, G.S., Ayed, A., Bochkareva, E., Bochkarev, A., and Arrowsmith, C.H. (2006) p53 transcriptional activation domain: A molecular chameleon? *Cell Cycle*, 5, 489–494.

140. Iwafuchi, M., Cuesta, I., Donahue, G., Takenaka, N., Osipovich, A.B., Magnuson, M.A., Roder, H., Seeholzer, S.H., Santisteban, P., and Zaret, K.S. (2020) Gene network transitions in embryos depend upon interactions between a pioneer transcription factor and core histones. *Nat. Genet.*, 52, 418–427.

141. Thompson, R.F., Walker, M., Siebert, C.A., Muench, S.P., and Ranson, N.A. (2016) An introduction to sample preparation and imaging by cryo-electron microscopy for structural biology. *Methods*, 100, 3–15.

142. Nagaich, A.K., Walker, D.A., Wolford, R., and Hager, G.L. (2004) Rapid periodic binding and displacement of the glucocorticoid receptor during chromatin remodeling. *Mol. Cell*, 14, 163–174.

143. Sekiya, T., Muthurajan, U.M., Luger, K., Tulin, A. V., and Zaret, K.S. (2009) Nucleosome-binding affinity as a primary determinant of the nuclear mobility of the pioneer transcription factor FoxA. *Genes Dev.*, 23, 804–809.

144. Nagaich, A.K., Rayasam, G. V., Martinez, E.D., Becker, M., Qiu, Y., Johnson, T.A., Elbi, C., Fletcher, T.M., John, S., and Hager, G.L. (2004) Subnuclear trafficking and gene targeting by steroid receptors. In *Annals of the New York Academy of Sciences*.Vol. 1024, pp. 213–220.

145. Boller, S., Ramamoorthy, S., Akbas, D., Nechanitzky, R., Burger, L., Murr, R., Schübeler, D., and Grosschedl, R. (2016) Pioneering Activity of the C-Terminal Domain of EBF1 Shapes the Chromatin Landscape for B Cell Programming. *Immunity*, 44, 527–541.

146. Nishimura, M., Arimura, Y., Nozawa, K., and Kurumizaka, H. (2020) Linker DNA and histone contributions in nucleosome binding by p53. *J. Biochem.*, 168, 669–675.

147. Lee, D., Kim, J.W., Seo, T., Hwang, S.G., Choi, E.J., and Choe, J. (2002) SWI/SNF complex interacts with tumor suppressor p53 and is necessary for the activation of p53-mediated transcription. *J. Biol. Chem.*, 277, 22330–22337.

148. Su, D., Wang, X., Campbell, M.R., Song, L., Safi, A., Crawford, G.E., and Bell, D.A. (2015) Interactions of chromatin context, binding site sequence content, and sequence evolution in stress-induced p53 occupancy and transactivation. *PLoS Genet.*, 11, e1004885.

149. Freewoman, J.M., Snape, R., and Cui, F. (2021) Temporal gene regulation by p53 is associated with the rotational setting of its binding sites in nucleosomes. *Cell Cycle*, 20, 792–807.

150. Schones, D.E., Cui, K., Cuddapah, S., Roh, T.Y., Barski, A., Wang, Z., Wei, G., and Zhao, K. (2008) Dynamic Regulation of Nucleosome Positioning in the Human Genome. *Cell*, 132, 887–898.

151. Giaimo, B.D., Ferrante, F., Herchenröther, A., Hake, S.B., and Borggrefe, T. (2019) The histone variant H2A.Z in gene regulation. *Epigenetic Chromatin*, 12, 37.

152. Kagawa, W., and Kurumizaka, H. (2021) Structural basis for DNA sequence recognition by pioneer factors in nucleosomes. *Curr. Opin. Struct. Biol.*, 71, 59–64.

153. Michael, A.K., and Thomä, N.H. (2021) Reading the chromatinized genome. *Cell*, 184, 3599–3611.

154. Tanaka, H., Takizawa, Y., Takaku, M., Kato, D., Kumagawa, Y., Grimm, S.A., Wade, P.A., and Kurumizaka, H. (2020) Interaction of the pioneer transcription factor GATA3 with nucleosomes. *Nat. Commun.*, 11, 4136.

155. Dodonova, S.O., Zhu, F., Dienemann, C., Taipale, J., and Cramer, P. (2020) Nucleosome-bound SOX2 and SOX11 structures elucidate pioneer factor function. *Nature*, 580, 669–672.

156. Michael, A.K., Grand, R.S., Isbel, L., Cavadini, S., Kozicka, Z., Kempf, G., Bunker, R.D., Schenk, A.D., Graff-Meyer, A., Pathare, G.R., *et al.* (2020) Mechanisms of OCT4-SOX2 motif readout on nucleosomes. *Science*, 368, 1460–1465.

Original paper

Nishimura Masahiro, Yasuhiro Arimura, Kayo Nozawa, and Hitoshi Kurumizaka

"Linker DNA and histone contribution in nucleosome binding by p53"

Journal of Biochemistry, 2020 Dec 26;168(6):669-675. doi: 10.1093/jb/mvaa081.

Acknowledgments

First, I would like to express my greatest appreciation to Dr. Hitoshi Kurumizaka for his supervision throughout my path across under graduated and graduate schools. Since I participated in Kurumizaka-lab, I have been fascinated by the mysteries of chromatin structure and function. I will forever be honored to have been trained in this incredibly enriching environment that he has established.

I sincerely appreciate all past and present members in Kurumizaka-lab for their cooperation and helpful discussions. Notably, I would like to thank: Dr. Yoshimasa Takizawa for his expert advice and support on the cryo-EM analysis, Dr. Kayo Nozawa for her considerate advice regarding the experiments and coaching of scientific writing, and Dr. Yasuhiro Arimura for his indispensable teaching of basic biochemical experiments, reading scientific papers, and oral presentation during my early years in Kurumizaka-lab. In addition, I am deeply thankful to Ms. Yukari Iikura, Ms. Yasuko Takeda, Ms. Yumi Shigematsu, and Dr. Mariko Dacher for their excellent assistance with countless stuff including experiments, paperwork, accounting, and so on.

I am deeply grateful for the financial support provided by Japan Society for the Promotion of Science (JSPS).

To end this doctoral thesis, I would like to express grateful feelings to my family for their continuous support and encouragement throughout my life.

Masahiro Nishimura